Enzymatic activities of all four respiratory chain complexes were decreased by loss of PINK1 (Fig. 2), with a dramatic reduction in complexes I and III activities in *PINK1*$^{-/-}$ MEFs.

3.2.1. Protein quantity of each respiratory chain complex

Decreased enzymatic activities per mitochondrial protein (Fig. 2) may be due to a decreased respiratory chain complex content per mitochondrial protein, or decreased enzymatic activities of each complex, or both. To assess these possibilities, we separated respiratory chain complexes in enzymatically active forms using BN-PAGE [30], and then detected each complex by immunoblotting (Fig. 3). Protein contents of all four respiratory chain complexes were decreased by loss of PINK1. In particular, complexes I and III contents were dramatically reduced in *PINK1*$^{-/-}$ MEFs. As the respiratory complex contents are in good agreement with their enzymatic activities, it is conceivable that decreased enzymatic activities per mitochondrial protein are not due to decreased enzymatic activities of each complex, but to decreased respiratory chain complex content per mitochondrial protein.

As complex I inhibitors such as MPTP and rotenone can cause parkinsonian symptoms in human and animal models, complex I defects are thought to be one of the main factors of PD pathogenesis [5,17,20]. According to recent reports, PINK1 is needed to maintain complex I activity through NdufA10 phosphorylation [21] and PINK1 deficiency can be rescued by Ndi1p, a yeast NADH:ubiquinone oxidoreductase that can bypass complex I [29]. In this study, we show that not only complex I but also complex III are deficient in *PINK1*$^{-/-}$ MEFs. Combined complexes I and III deficiencies were previously reported in patients harboring mutations in the *NDUFS4* gene of complex I [6], or the *MT-CYB* gene of complex III [16]. These are presumably due to respiratory chain supercomplexes, large assemblies of respiratory chain complexes with small electron carriers for stabilization and enhancement of electron transport [18,23]. Studies on the supercomplex status of *PINK1*$^{-/-}$ MEFs are under way.

Acknowledgements

This work was supported by Grant-in-Aid for Young Scientists (T.A.) and for Challenging Exploratory Research (S. Saiki) from JSPS, and grants from the Kanagawa Nanbyo Study Foundation (T.A.) and the Takeda Scientific Foundation (S. Saiki). We thank Drs. Clement Gautier and Jie Shen (Harvard Medical School, Boston, MA, USA) for providing *PINK1* knock-out mice, Dr. Noriyuki Matsuda (Tokyo Metropolitan Institute of Medical Science, Tokyo, Japan) for assistance to obtain immortalized cells, Dr. Takashi Ueno (Juntendo University, Tokyo, Japan) for providing anti-ATP synthase subunit β antibody, and Dr. Dongchon Kang (Kyushu University, Fukuoka, Japan) for providing anti-TFAM antibody.

References

[1] P.M. Abou-Sleiman, M.M. Muqit, N.W. Wood, Expanding insights of mitochondrial dysfunction in Parkinson's disease, Nat. Rev. Neurosci. 7 (2006) 207–219.
[2] T. Amo, M.D. Brand, Were inefficient mitochondrial haplogroups selected during migrations of modern humans? A test using modular kinetic analysis of coupling in mitochondria from cybrid cell lines, Biochem. J. 404 (2007) 345–351.
[3] T. Amo, S. Sato, S. Saiki, A.M. Wolf, M. Toyomizu, C.A. Gautier, J. Shen, S. Ohta, N. Hattori, Mitochondrial membrane potential decrease caused by loss of PINK1 is not due to proton leak, but to respiratory chain defects, Neurobiol. Dis. 41 (2011) 111–118.
[4] M.A. Birch-Machin, D.M. Turnbull, Assaying mitochondrial respiratory complex activity in mitochondria isolated from human cells and tissues, Methods Cell Biol. 65 (2001) 97–117.
[5] J. Blesa, S. Phani, V. Jackson-Lewis, S. Przedborski, Classic and new animal models of Parkinson's disease, J. Biomed. Biotechnol. 2012 (2012) 845618.
[6] S.M. Budde, L.P. van den Heuvel, A.J. Janssen, R.J. Smeets, C.A. Buskens, L. DeMeirleir, R. Van Coster, M. Baethmann, T. Voit, J.M. Trijbels, J.A. Smeitink, Combined enzymatic complex I and III deficiency associated with mutations in the nuclear encoded NDUFS4 gene, Biochem. Biophys. Res. Commun. 275 (2000) 63–68.
[7] C.T. Chu, P.I.N.K1. Tickled, Mitochondrial homeostasis and autophagy in recessive Parkinsonism, Biochim. Biophys. Acta 1802 (2010) 20–28.
[8] I.E. Clark, M.W. Dodson, C. Jiang, J.H. Cao, J.R. Huh, J.H. Seol, S.J. Yoo, B.A. Hay, M. Guo, Drosophila pink1 is required for mitochondrial function and interacts genetically with *parkin*, Nature 441 (2006) 1162–1166.
[9] N. Exner, A.K. Lutz, C. Haass, K.F. Winklhofer, Mitochondrial dysfunction in Parkinson's disease: molecular mechanisms and pathophysiological consequences, EMBO J. 31 (2012) 3038–3062.
[10] C.A. Gautier, T. Kitada, J. Shen, Loss of PINK1 causes mitochondrial functional defects and increased sensitivity to oxidative stress, Proc. Natl. Acad. Sci. U.S.A. 105 (2008) 11364–11369.
[11] M.E. Gegg, J.M. Cooper, A.H. Schapira, J.W. Taanman, Silencing of PINK1 expression affects mitochondrial DNA and oxidative phosphorylation in dopaminergic cells, PLoS ONE 4 (2009) e4756.
[12] N. Hattori, M. Tanaka, T. Ozawa, Y. Mizuno, Immunohistochemical studies on complexes I, II, III, and IV of mitochondria in Parkinson's disease, Ann. Neurol. 30 (1991) 563–571.
[13] H.H. Hoepken, S. Gispert, B. Morales, O. Wingerter, D. Del Turco, A. Mulsch, R.L. Nussbaum, K. Muller, S. Drose, U. Brandt, T. Deller, B. Wirth, A.P. Kudin, W.S. Kunz, G. Auburger, Mitochondrial dysfunction, peroxidation damage and changes in glutathione metabolism in PARK6, Neurobiol. Dis. 25 (2007) 401–411.
[14] D. Kang, S.H. Kim, N. Hamasaki, Mitochondrial transcription factor A (TFAM): roles in maintenance of mtDNA and cellular functions, Mitochondrion 7 (2007) 39–44.
[15] D.M. Kirby, D.R. Thorburn, D.M. Turnbull, R.W. Taylor, Biochemical assays of respiratory chain complex activity, Methods Cell Biol. 80 (2007) 93–119.
[16] E. Lamantea, F. Carrara, C. Mariotti, L. Morandi, V. Tiranti, M. Zeviani, A novel *nonsense mutation (Q352X) in the mitochondrial cytochrome b gene* associated with a combined deficiency of complexes I and III, Neuromuscul. Disord. 12 (2002) 49–52.
[17] J.W. Langston, P. Ballard, J.W. Tetrud, I. Irwin, Chronic Parkinsonism in humans due to a product of meperidine-analog synthesis, Science 219 (1983) 979–980.
[18] E. Lapuente-Brun, R. Moreno-Loshuertos, R. Acin-Perez, A. Latorre-Pellicer, C. Colas, E. Balsa, E. Perales-Clemente, P.M. Quiros, E. Calvo, M.A. Rodriguez-Hernandez, P. Navas, R. Cruz, A. Carracedo, C. Lopez-Otin, A. Perez-Martos, P. Fernandez-Silva, E. Fernandez-Vizarra, J.A. Enriquez, Supercomplex assembly determines electron flux in the mitochondrial electron transport chain, Science 340 (2013) 1567–1570.
[19] N. Matsuda, S. Sato, K. Shiba, K. Okatsu, K. Saisho, C.A. Gautier, Y.S. Sou, S. Saiki, S. Kawajiri, F. Sato, M. Kimura, M. Komatsu, N. Hattori, K. Tanaka, PINK1 stabilized by mitochondrial depolarization recruits Parkin to damaged mitochondria and activates latent Parkin for mitophagy, J. Cell Biol. 189 (2010) 211–221.
[20] Y. Mizuno, T. Saitoh, N. Sone, Inhibition of mitochondrial NADH-ubiquinone oxidoreductase activity by 1-methyl-4-phenylpyridinium ion, Biochem. Biophys. Res. Commun. 143 (1987) 294–299.
[21] V.A. Morais, D. Haddad, K. Craessaerts, P.J. De Bock, J. Swerts, S. Vilain, L. Aerts, L. Overbergh, A. Grunewald, P. Seibler, C. Klein, K. Gevaert, P. Verstreken, B. De Strooper, PINK1 loss of function mutations affect mitochondrial complex I activity via NdufA10 ubiquinone uncoupling, Science 344 (2014) 203–207.
[22] V.A. Morais, P. Verstreken, A. Roethig, J. Smet, A. Snellinx, M. Vanbrabant, D. Haddad, C. Frezza, W. Mandemakers, D. Vogt-Weisenhorn, R. Van Coster, W. Wurst, L. Scorrano, B. De Strooper, Parkinson's disease mutations in PINK1 result in decreased Complex I activity and deficient synaptic function, EMBO Mol. Med. 1 (2009) 99–111.
[23] D. Moreno-Lastres, F. Fontanesi, I. Garcia-Consuegra, M.A. Martin, J. Arenas, A. Barrientos, C. Ugalde, Mitochondrial complex I plays an essential role in human respirasome assembly, Cell Metabolism 15 (2012) 324–335.
[24] D. Narendra, A. Tanaka, D.F. Suen, R.J. Youle, Parkin is recruited selectively to impaired mitochondria and promotes their autophagy, J. Cell Biol. 183 (2008) 795–803.
[25] J. Park, S.B. Lee, S. Lee, Y. Kim, S. Song, S. Kim, E. Bae, J. Kim, M. Shong, J.M. Kim, J. Chung, Mitochondrial dysfunction in *Drosophila PINK1* mutants is complemented by *parkin*, Nature 441 (2006) 1157–1161.
[26] C. Piccoli, M. Ripoli, G. Quarato, R. Scrima, A. D'Aprile, D. Boffoli, M. Margaglione, C. Criscuolo, G. De Michele, A. Sardanelli, S. Papa, N. Capitanio, Coexistence of mutations in *PINK1* and mitochondrial DNA in early onset parkinsonism, J. Med. Genet. 45 (2008) 596–602.
[27] J.W. Pridgeon, J.A. Olzmann, L.S. Chin, L. Li, PINK1 protects against oxidative stress by phosphorylating mitochondrial chaperone TRAP1, PLoS Biol. 5 (2007) e172.
[28] E.M. Valente, P.M. Abou-Sleiman, V. Caputo, M.M. Muqit, K. Harvey, S. Gispert, Z. Ali, D. Del Turco, A.R. Bentivoglio, D.G. Healy, A. Albanese, R. Nussbaum, R. González-Maldonado, T. Deller, S. Salvi, P. Cortelli, W.P. Gilks, D.S. Latchman, R.J. Harvey, B. Dallapiccola, G. Auburger, N.W. Wood, Hereditary early-onset Parkinson's disease caused by mutations in *PINK1*, Science 304 (2004) 1158–1160.
[29] S. Vilain, G. Esposito, D. Haddad, O. Schaap, M.P. Dobreva, M. Vos, S. Van Meensel, V.A. Morais, B. De Strooper, P. Verstreken, The yeast complex I equivalent NADH dehydrogenase rescues *pink1* mutants, PLoS Genet. 8 (2012) e1002456.
[30] I. Wittig, H.P. Braun, H. Schägger, Blue native PAGE, Nat. Protoc. 1 (2006) 418–428.

Archival Report

Biological Psychiatry

Utility of Scalp Hair Follicles as a Novel Source of Biomarker Genes for Psychiatric Illnesses

Motoko Maekawa, Kazuo Yamada, Manabu Toyoshima, Tetsuo Ohnishi, Yoshimi Iwayama, Chie Shimamoto, Tomoko Toyota, Yayoi Nozaki, Shabeesh Balan, Hideo Matsuzaki, Yasuhide Iwata, Katsuaki Suzuki, Mitsuhiro Miyashita, Mitsuru Kikuchi, Motoichiro Kato, Yohei Okada, Wado Akamatsu, Norio Mori, Yuji Owada, Masanari Itokawa, Hideyuki Okano, and Takeo Yoshikawa

ABSTRACT

BACKGROUND: Identifying beneficial surrogate genetic markers in psychiatric disorders is crucial but challenging.

METHODS: Given that scalp hair follicles are easily accessible and, like the brain, are derived from the ectoderm, expressions of messenger RNA (mRNA) and microRNA in the organ were examined between schizophrenia (*n* for first/second = 52/42) and control subjects (*n* = 62/55) in two sets of cohort. Genes of significance were also analyzed using postmortem brains (*n* for case/control = 35/35 in Brodmann area 46, 20/20 in cornu ammonis 1) and induced pluripotent stem cells (*n* = 4/4) and pluripotent stem cell-derived neurospheres (*n* = 12/12) to see their role in the central nervous system. Expression levels of mRNA for autism (*n* for case/control = 18/24) were also examined using scalp hair follicles.

RESULTS: Among mRNA examined, *FABP4* was downregulated in schizophrenia subjects by two independent sample sets. Receiver operating characteristic curve analysis determined that the sensitivity and specificity were 71.8% and 66.7%, respectively. *FABP4* was expressed from the stage of neurosphere. Additionally, microarray-based microRNA analysis showed a trend of increased expression of *hsa-miR-4449* ($p = .0634$) in hair follicles from schizophrenia. *hsa-miR-4449* expression was increased in Brodmann area 46 from schizophrenia ($p = .0007$). Finally, we tested the expression of nine putative autism candidate genes in hair follicles and found decreased *CNTNAP2* expression in the autism cohort.

CONCLUSIONS: Scalp hair follicles could be a beneficial genetic biomarker resource for brain diseases, and further studies of *FABP4* are merited in schizophrenia pathogenesis.

Keywords: Autism, *CNTNAP2*, FABP4, *hsa-miR-4449*, MicroRNA, Schizophrenia

http://dx.doi.org/10.1016/j.biopsych.2014.07.025

The disease mechanisms underlying psychiatric illnesses remain largely undetermined. Great efforts have gone into identifying novel biomarkers that would assist in the development of objective diagnostic tools and novel therapeutic and prophylactic interventions, as well as facilitate the subdivision of disease states, based on pathogenesis, for optimal drug selection. There are, however, major obstacles in the search for novel biomarkers, primarily the difficulty in obtaining brain tissue from living donors and the lack of accurate experimental animal models. Brain is an ectodermal tissue and shares its developmental origins with scalp hair follicles, which are readily accessible miniorgans within the skin. Despite their shared embryonic origins, hair follicles have not previously been utilized as a bio-resource in the hunt for proxy genes in psychiatric diseases. In the current study, we first examined whether schizophrenia-relevant genes, namely those related to the γ-aminobutyric acid (GABA)ergic system (1–3), myelin (3–5), and fatty acids (6–11), are expressed in hair follicles and if expressed whether expression is differential between cases and control subjects, using an exploratory sample set. Next, we attempted to validate any differential expression and examine the effects of potential confounding factors using a second independent sample set. We then analyzed the identified biomarker candidate *FABP4*/fatty acid binding protein 4 (FABP4) expression in serum, postmortem brain samples, induced pluripotent stem cells (iPSCs), and iPSC-derived neurospheres. In addition to messenger RNA (mRNA), we also examined the expression levels of microRNA (miRNA) in hair follicles, postmortem brains, iPSCs, and iPSC-derived neurosphere samples from patients with schizophrenia and control subjects. Lastly, we tested candidate gene expression in hair follicles from patients with autism. Based on the results of our comprehensive analysis, we proposed scalp hair follicles as a beneficial genetic resource for schizophrenia and autism in the search for potential biomarkers.

ISSN: 0006-3223

Biological Psychiatry ▮▮▮, 2014; ▮:▮▮▮–▮▮▮ www.sobp.org/journal

METHODS AND MATERIALS

Scalp Hair Follicle Samples

All samples were collected from ethnic Japanese within Japan. The first set of exploratory scalp hair follicle samples for schizophrenia and control subjects was derived from residents in the northern district of Kanto, while the confirmatory second set came from the Tokyo area. Diagnoses were made by at least two experienced psychiatrists, using DSM-IV criteria. Demographic data for scalp hair follicle samples derived from schizophrenia are described in Table 1. The scalp hair follicle samples from autism participants and control subjects were collected from the Chubu area. The diagnosis of autism spectrum disorder was made using the DSM-IV-TR criteria. We then administered the Autism Diagnostic Interview-Revised (ADI-R) (12) to 14 of 18 cases and made a confirmed diagnosis of autism for those 14 cases. Interviews for the ADI-R were conducted by experienced child psychiatrists who are licensed to use the Japanese version of the ADI-R (13). Demographic data relating to scalp hair follicle samples for autism are described in Table 1.

RNA Extraction and Quantification

Ten hairs were plucked from the scalp of each subject using forceps. The hairs were checked for the presence of a sheath. Hairs were trimmed to approximately 1.5 cm in length, containing the bulb region, and dropped into a 1.5 mL microfuge tube (BM Equipment, Tokyo, Japan) containing RNAlater solution (Ambion, Grand Island, New York). Total RNA was extracted using the RNAqueous-Micro kit (Ambion). Single-stranded complementary DNA (cDNA) was synthesized using SuperScript VILO Master Mix (Invitrogen, Grand Island, New York). Quantitative reverse-transcription PCR (qRT-PCR) analysis of mRNAs was conducted using an ABI7900HT Fast Real-Time PCR System (Applied Biosystems, Grand Island, New York). TaqMan probes were TaqMan Gene Expression Assays products (Applied Biosystems). All qRT-PCR data were captured using the SDS v2.4 (Applied Biosystems). The ratios of relative concentrations of target molecules to the *GAPDH* gene (target molecule/*GAPDH* gene) were calculated. All reactions were performed in triplicate based on the standard curve method.

Statistical Analysis

We used the interquartile range to find outliers. The differences between the 25th (quartile 1) and 75th percentiles (quartile 3) were used to identify extreme values (outliers) in the tails of the distribution. Statistical evaluation was performed by Mann-Whitney *U* test for means between patient and control groups and by Spearman's R test for correlation using SPSS software version 19 (IBM, Tokyo, Japan).

Analyses of miRNA Expressions and Potential Targets of miRNAs

For microarray-based miRNA analysis, we used the miRBase Rel. 18.0 platform (Agilent Technologies, Santa Clara California), capable of measuring 1919 human mature miRNAs in the age-/sex-matched subset of the first hair follicle sample set (Table S1 in Supplement 1). The miRNAs were labeled using the miRNA Complete Labeling Reagent and Hyb Kit (Agilent Technologies) and hybridized to the arrays. Images were scanned with a High-Resolution C scanner (Agilent Technologies) and analyzed using GeneSpring GX (Agilent Technologies). Comparisons of miRNA expression values between schizophrenia and control groups were performed using GeneSpring 12.6 (Agilent Technologies). To normalize the intermicroarray range of expression intensities, the percentile shift method (90th percentile) was used. The genes whose expression data were available in more than 50% of hybridizations were statistically evaluated between schizophrenia and control groups using the two-tailed Mann-Whitney *U* test. For quantification of individual miRNAs, we performed TaqMan-based miRNA qRT-PCR (Applied Biosystems, Grand Island, New York) according to the manufacturer's instructions, using *U6 snRNA* as a control probe. All reactions for miRNA quantification were also performed in triplicate, based on the standard curve method. Statistical evaluation methods were the same as those for mRNA.

Table 1. Demographic Characteristics of Hair Follicle Sample Sets

	Control Subjects	Patients	*p* Value
First Sample Set for Schizophrenia			
n	62	52	
Sex (female/male)	41 / 21	25 / 27	.0518[a]
Age (mean ± SD)	41.26 ± 12.26	50.98 ± 10.86	<.0001[b]
Second Sample Set for Schizophrenia			
n	55	42	
Sex (female/male)	26 / 29	20 / 22	.973[a]
Age (mean ± SD)	46.87 ± 13.56	49.93 ± 12.97	.2777[b]
Duration of illness (mean ± SD)		22.79 ± 14.66	
Autism Sample Set			
n	24	18	
Sex (female/male)	24 / 0	16 / 2	.1777[a]
Age (mean ± SD)	32.60 ± 3.91	25.61 ± 4.95	<.0001[b]

[a]Evaluated by chi-square test.
[b]Evaluated by two-tailed *t* test.

To identify the potential targets of a specific miRNA, we performed in silico analysis using web-based miRNA target prediction methods, TargetScan (http://www.targetscan.org, Release 6.2; Whitehead Institute for Biomedical Research, Cambridge, Massachusetts) and miRDB (http://mirdb.org/miRDB/; Washington University School of Medicine, St. Louis, Missouri).

Immunohistochemistry

The plucked hairs were rinsed briefly in phosphate-buffered saline and dropped into a 1.5 mL microfuge tube containing 1 mL of 10% neutral-buffered formalin (4°C, 1 hour). The fixed hairs were pre-embedded in 4% agarose (Sigma-Aldrich, St Louis, Missouri) in phosphate-buffered saline, pH 7.4. At this point, it was possible to orientate the hairs into their desired position for either longitudinal or transverse sectioning. Blocks were embedded in capsules, which were filled with O.C.T. compound (Sakura Finetek, Tokyo, Japan). Cryostat sections (8 μm thick) of plucked hair follicles were processed for immunohistochemistry. The sections were blocked with 10% goat serum in .05 mol/L Tris buffered saline plus .05% Tween 20 (TBST), followed by three rinses in TBST (20 min each). The primary antibodies were applied for overnight at 4°C. After three washes in TBST (20 min each), secondary antibodies were applied to sections at room temperature (1 hour). Slides were counterstained with 4',6-diamidino-2-phenylindole to highlight nuclei. After washing in TBST, the slides were mounted in PermaFluor Aqueous Mounting Medium (Thermo Fisher Scientific, Waltham, Massachusetts). Fluorescent signals were detected using a confocal laser-scanning microscope FV1000 (Olympus, Tokyo, Japan).

Antibodies

See Supplementary Methods and Materials in Supplement 1.

Analysis of FABP4 Protein Levels in Serum

See Supplementary Methods and Materials in Supplement 1.

Postmortem Brain Analysis

See Supplementary Methods and Materials in Supplement 1.

Establishment of iPSC Lines

Dermal fibroblasts (human dermal fibroblasts) from the facial dermis of a 36-year-old Caucasian female subject (Cell Applications, Inc., San Diego, California) were used to establish control iPSCs 201B7 and YA9 (14). The remaining control iPSCs, WD39 and KA23, were generated from a 16-year-old Japanese female subject (15) and a 40-year-old Japanese male subject (Matsumoto, Ph.D., *et al.*, personal communication, 2013), respectively. The 201B7 iPSCs were kindly provided by Yamanaka, M.D., Ph.D., Kyoto University (14). The iPSCs YA9, WD39, and KA23 have been described in a previous report (15). The schizophrenia derived iPSCs from patients with 22q11.2 deletions SA001 and KO001 were generated from Japanese female subjects aged 37 and 30 years old, respectively (see Clinical History in Supplement 1).

The maintenance of human dermal fibroblasts, lentiviral production, retroviral production, infection, stem cell culture, and characterization were performed as described previously (15).

In Vitro Neural Differentiation of Induced Pluripotent Stem Cells

The iPSCs were plated in T75 flasks after dissociation into single cells and cultured for 14 days in neural culture medium supplemented with leukemia inhibitory factor (Merck Millipore, Darmstadt, Germany) and basic fibroblast growth factor (Peprotech, Rocky Hill, New Jersey). Neurospheres were passaged repeatedly by culturing in the same manner (16,17).

Comparative Genomic Hybridization Array Analysis

See Supplementary Methods and Materials in Supplement 1.

Ethical Issues

This study was approved by the Ethics Committees of RIKEN and all participating institutes, including the Keio University School of Medicine, an ethical committee for skin biopsy and iPSC production (approval No. 20080016), and conducted according to the principles expressed in the Declaration of Helsinki. All control subjects and patients gave informed, written consent to participate in the study after being provided with and receiving an explanation of study protocols and objectives.

RESULTS

Expression of mRNA in Scalp Hair Follicles from Schizophrenia and Control Subjects

Gene expression profiles of schizophrenia postmortem brains have been well studied. However, studies have been hampered by uncontrollable confounding factors associated with postmortem brains and an inaccessibility of brain tissue from living donors. Therefore, we set out to analyze gene expression in hair follicles. Previous studies provide substantial support for reduced expression of genes related to oligodendrocyte and GABAergic systems in schizophrenia pathology (1–4). In addition, our (6,7,9) and other studies (8,10,11) on *FABPs* (genes for fatty acid binding proteins) raise the possibility of disturbed lipid metabolism in the susceptibility to this disease. Based on these findings, we selected 22 genes: 8 from the GABAergic system, 9 with myelin relevance, and 5 with lipid relevance (Table 2). The amount of mRNA from an individual subject's hair follicles was not enough for a systemic cDNA microarray. We used *GAPDH* as an internal control. An exploratory scalp hair follicle sample panel (the first sample set) consisted of samples from 52 patients with schizophrenia and 62 control subjects (Table 1). qRT-PCR analysis showed that seven genes, namely *CALB2*, *SST*, *CNP*, *PMP22*, *FABP4*, *FABP7,* and *FAAH* were differentially expressed ($p < .05$) in samples from schizophrenia compared with control subjects (Table 2; Figure S1 in Supplement 1).

To replicate the finding, we examined the expression levels of these seven genes using an age-/sex-matched, independent confirmatory set (a second sample set) composed of 42 patients with schizophrenia and 55 control subjects (Table 1). Of the seven genes, only *FABP4* showed significantly decreased expression (an average reduction of 43% compared with a reduction of 40% in the first set of samples) in schizophrenia samples (Figure 1A; Table 2). Correlation analyses demonstrated no significant effects for age, dose of

Table 2. List of Examined Genes and Their Expression in the First and Second Scalp Hair Follicle Sample Sets from Schizophrenia

			First Sample Set			Second Sample Set		
			Mean ± SD of Corresponding Gene / *GAPDH*			Mean ± SD of Corresponding Gene / *GAPDH*		
Gene Category	Gene Symbol	Assay ID[a]	Control (n = 62)	Schizophrenia (n = 49)	p Value[b]	Control (n = 62)	Schizophrenia (n = 49)	p Value[b]
GABAergic System	*GAD1*	Hs01065893_m1	.881 ± .598	1.119 ± .707	.118			
	GAD2	Hs00609534_m1	Not detectable					
	GABRA1	Hs00168058_m1	2.347 ± 2.761	.832 ± .964	.378			
	GABRD	Hs00181309_m1	1.055 ± .758	.945 ± .618	.666			
	SLC6A1	Hs01104475_m1	1.047 ± .830	.985 ± .555	.682			
	PVALB	Hs00161045_m1	1.067 ± .569	1.074 ± .669	.87			
	CALB2	Hs00418693_m1	1.024 ± .355	1.163 ± .303	.037[d]	.715 ± .373	.857 ± .300	.095[c]
	SST	Hs00356144_m1	.626 ± .549	1.052 ± .923	.028[d]	.910 ± .683	1.812 ± 1.802	.151[c]
Myelin Relevance	*APC*	Hs01568269_m1	1.001 ± .243	.939 ± .233	.131			
	CLDN11	Hs00194440_m1	.860 ± .605	.984 ± .854	.862			
	CNP	Hs00263981_m1	1.148 ± .336	.985 ± .186	.002[d]	.928 ± .415	1.052 ± .210	.456
	CSPG4	Hs00361541_g1	.976 ± .536	1.050 ± .364	.252			
	MAG	Hs01114387_m1	Not detectable					
	NES	Hs00707120_s1	1.018 ± .496	1.013 ± .403	.98			
	OLG2	Hs00300164_s1	Not detectable					
	PMP22	Hs00165556_m1	1.006 ± .370	.804 ± .261	.003[d]	.807 ± .410	.844 ± .400	.987
	SOX10	Hs00366918_m1	1.072 ± .748	.984 ± .508	.99			
Lipid Relevance	*FABP3*	Hs00997360_m1	.763 ± .486	.807 ± .372	.292			
	FABP4	Hs01086177_m1	1.050 ± .470	.653 ± .251	<.0001[d]	1.138 ± .708	.650 ± .232	**<.001**
	FABP5	Hs02339439_g1	1.118 ± .215	1.084 ± .179	.312			
	FABP7	Hs00361426_m1	.562 ± .332	1.018 ± .744	.003[d]	.519 ± .372	.530 ± .355	.754
	FAAH	Hs01038660_m1	1.008 ± .344	.857 ± .221	.013[d]	.836 ± .303	.753 ± .281	.180[c]
Control	*GAPDH*	Hs02758991_g1						

GABA, gamma-aminobutyric acid.

[a]Probe ID in TaqMan Gene Expression Assay system.

[b]Evaluated by two-tailed Mann-Whitney U test.

[c]For these analyses, only 49 control and 36 schizophrenia samples were available.

[d]Significant changes.

antipsychotics [haloperidol equivalent (18,19)], or duration of illness on the expression levels of *FABP4* (Figure S2A–C in Supplement 1). Since serum levels of Fabp4 were reported to be affected by nutritional fluctuations in mice (that is, suppressed by feeding) (20), we examined the effect of sampling time after the last meal on *FABP4* expression in hair follicles and found no significant change (Figure S2D in Supplement 1). Nor did we detect an effect for sex on *FABP4* levels: male control versus female control subjects, p = .950; male schizophrenia versus female schizophrenia subjects, p = .360; male (control + schizophrenia subjects) versus female (control + schizophrenia subjects), p = .387; all evaluated by the Mann-Whitney U test.

Circulating FABP4 is known to be associated with metabolic markers (21,22), so we examined the effects of weight, height, body mass index, and body fat percentage on *FABP4* expression in the second hair follicle sample set (Figure S3 in Supplement 1). None of these factors affected the expression ratios of *FABP4/GAPDH* in hair follicles. Despite the fact that olanzapine alters lipid metabolism (23,24), we detected no significant correlation between *FABP4* expression levels in hair follicles and olanzapine dose (mg/day) in the second set of schizophrenia samples (Spearman's rho = −.2289; 95% confidence interval = −.5258 to .1178; p = .180).

From these results, *FABP4* expression levels in hair follicles would appear to be a robust marker for schizophrenia. Receiver operating characteristic curve analysis determined an optimal cutoff level of .769, based on the minimum distance from the curve to upper left corner (= .191) and area under the curve = .713 (95% confidence interval = .609–.817) (Figure S4 in Supplement 1). With this cutoff level for the *FABP4/GAPDH* mRNA ratio, the sensitivity, specificity, and positive and negative predictive values were 71.8%, 66.7%, 60.9%, and 76.6%, respectively.

Immunohistochemical Analysis of FABP4 in Scalp Hair Follicles

Figure 2A shows the structure of a hair follicle (25,26). Moving inward, a plucked scalp hair consists of the following components: the outer root sheath, companion layer, inner root sheath (IRS), the cortex, and medullar. Each of these components has an epidermal origin and each compartment expresses specific genes from the keratin family (26) (Figure 2B). FABP4 is co-expressed with K71 in the IRS cuticle layer and displays partially overlapping expression with K85 in the cuticle, matrix/precortex, and mid/upper cortex (27). However, FABP4 shows scant co-expression with K14 in the outer root sheath layer (Figure 2C, D). These results indicate that FABP4 is expressed in the IRS and part of the hair cortex.

Expression of FABP4 in Serum and Postmortem Brains

We measured FABP4 protein levels in the same cohort as the second hair follicle sample, using an enzyme-linked immunosorbent assay kit, to see whether serum levels of FABP4 could

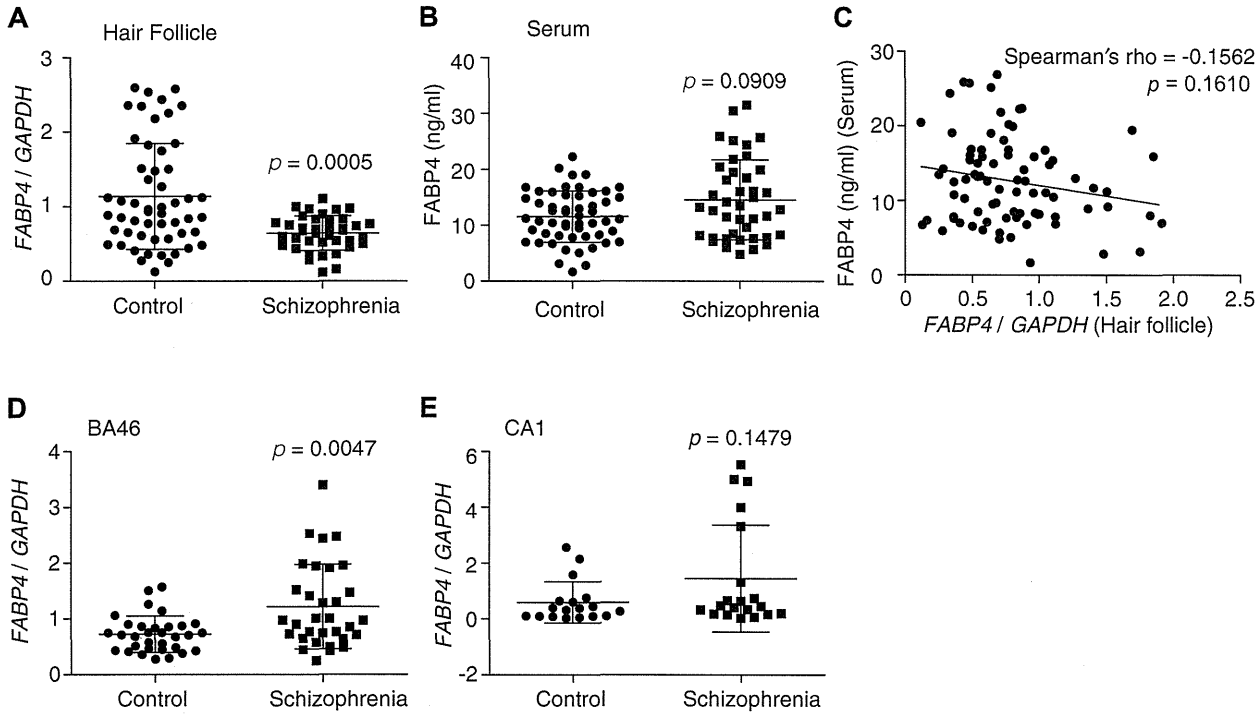

Figure 1. *FABP4*/fatty acid binding protein 4 (FABP4) expression analyses in schizophrenia and control samples. **(A, B, D, E)** Results for hair follicles (the second sample set), serum, and postmortem brain tissue (Brodmann area [BA]46 and cornu ammonis [CA]1) are shown. *GAPDH* was used as an internal control. *p* values were calculated using two-tailed Mann-Whitney *U* test. Horizontal bars show mean ± SD. **(C)** Correlations between relative *FABP4* expression levels in scalp hair follicles and FABP4 levels in serum are also shown. Statistical evaluations were performed using Spearman's rank correlation test.

also be a proxy for schizophrenia. However, the measure did not differ significantly between schizophrenia and control samples, although a trend of increase was seen in schizophrenia (Figure 1B). In addition, using the second sample cohort, there was no significant correlation between serum FABP4 and *FABP4* mRNA levels in hair follicles (Figure 1C). Interestingly, in contrast to findings in mice (20), serum FABP4 levels were not affected by time elapsed after the last meal in either disease or control groups (Figure S5 in Supplement 1).

In postmortem brains, *FABP4* transcript expression was significantly elevated in the frontal cortex (Brodmann area [BA]46) of schizophrenia compared with control samples (p = .0047) (Figure 1D), suggesting its role in schizophrenia pathophysiology. Expression of *FABP4* in hippocampus cornu ammonis 1 remained unchanged between schizophrenia and control samples (Figure 1E), implicating region specificity for the function of *FABP4* in schizophrenia. Both of these brain regions showed particularly high expression levels in four schizophrenia samples derived from patients not recorded to have taken particular therapeutic drugs (Table S3 in Supplement 1), although the possibility of drug effects cannot be excluded.

Expression Analysis of miRNAs in Scalp Hair Follicles and Postmortem Brains

We further performed microarray-based miRNA analysis and measured the expression levels of 1919 human mature miRNAs using the miRBase Release 18.0 platform (Agilent) in an age- and sex-matched subset of the first hair follicle sample set (Table S1 in Supplement 1). We detected three miRNAs, which satisfied our criteria of an absolute fold change (FC) (schizophrenia group/control group) ≥ 2 and $p < .05$ (by Mann-Whitney *U* test, two-tailed). These were *hsa-miR-4449* (FC = 3.45, p = .0032), *hsa-miR-1237* (FC = 2.55, p = .028), and *hsa-miR-4769-3p* (FC = 2.03, p = .028). In the next step, we tested these three miRNAs in the second hair follicle sample set (Table 1), using qRT-PCR, with U6 small nuclear RNA as a control probe. *hsa-miR-4449* showed a top hit with upregulation, although not to significant levels, in schizophrenia (FC = 1.25, p = .063) (Figure 3A).

In postmortem brains (BA46), *hsa-miR-4449* showed increased expression (p = .0007) in schizophrenia samples (Figure 3B), suggesting possible contribution of this gene also to schizophrenia.

Expression Analysis of *FABP4* and *hsa-miR-4449* in iPSCs and iPSC-Derived Neurospheres

Recently, iPSCs have been used for human disease modeling, particularly in neurological disorders (28–30). We have established iPSCs from control subjects (one line each from four subjects) and schizophrenia patients carrying a 22q11.2 microdeletion (two lines each from two patients) (31) (Figure 4). Then, we established three neurosphere lines from each iPSC line. We chose 22q11.2 deletion carriers for analysis (for comparative genomic hybridization array analysis using the iPSCs, see Supplementary Methods and Materials in Supplement 1), since the 22q11.2 deletion is a well-defined

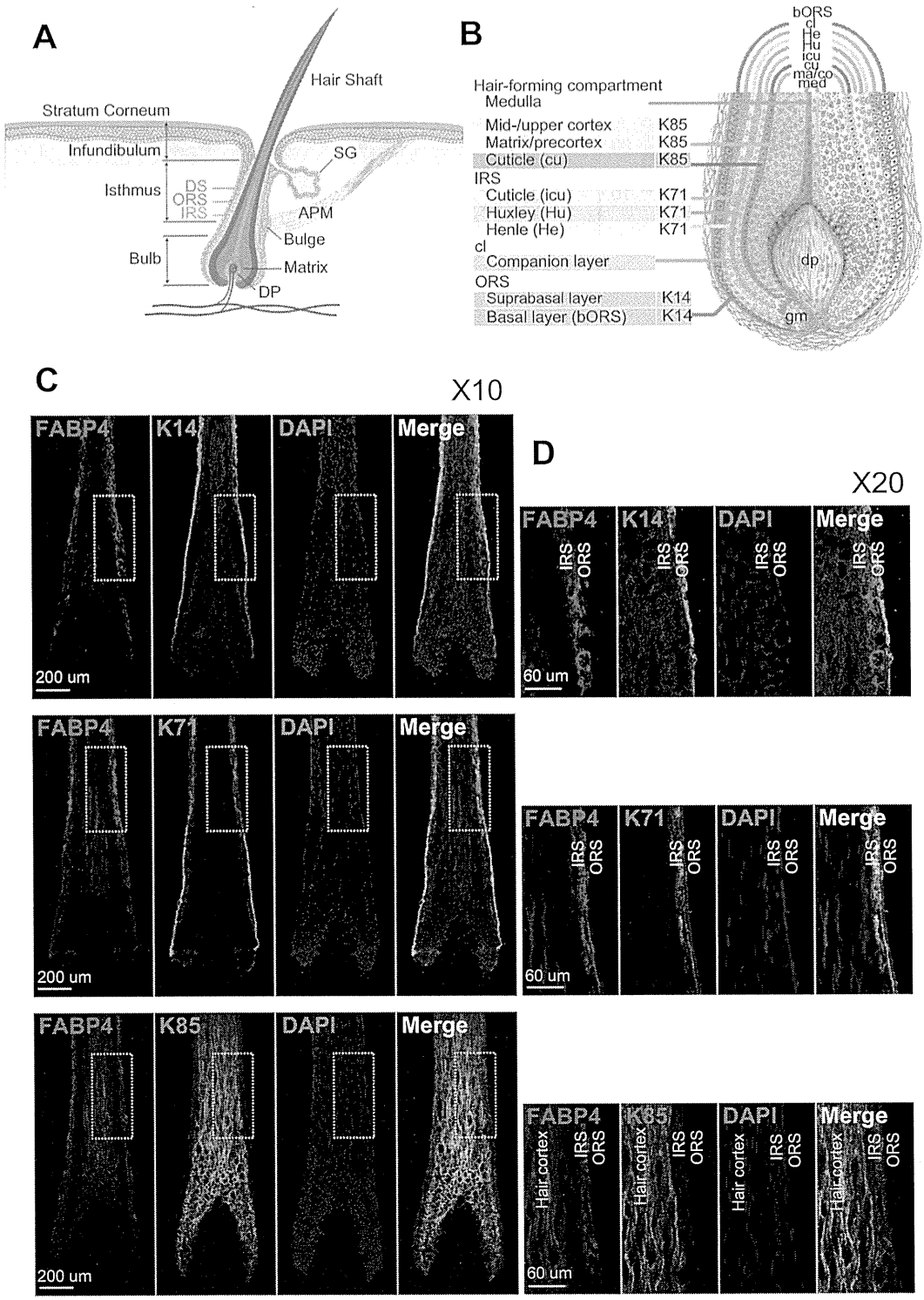

Figure 2. Expression patterns of fatty acid binding protein 4 (FABP4) in scalp hair follicles. **(A)** Schematic illustration showing the structure of hair follicles. **(B)** Schematic presentation of epithelial/hair keratin expression patterns. Keratin K71 is expressed in the three inner root sheath (IRS) layers, while K14 is known as outer root sheath (ORS) keratin. Keratin K85 is present in the hair-forming compartment. **(C)** Immunofluorescent labeling of FABP4 and hair keratins (K14, K71, and K85) in scalp hair follicles. K14 is uniformly expressed throughout the widely stratified follicular ORS. K71 is expressed in all compartments of the hair IRS. Keratin K85 expression extends from the hair matrix to the upper cortex and the hair cuticle. FABP4 is seen in the IRS and part of the hair cortex (merged green and red). 4',6-diamidino-2-phenylindole (DAPI) was used for nuclear staining. **(D)** Magnified picture of **(C)**. APM, arrector pili muscle; cl, companion layer; DP, dermal papilla; DS, dermal sheath; gm, germinative matrix; ma/co, matrix/precortex; med, medulla; SG, sebaceous gland.

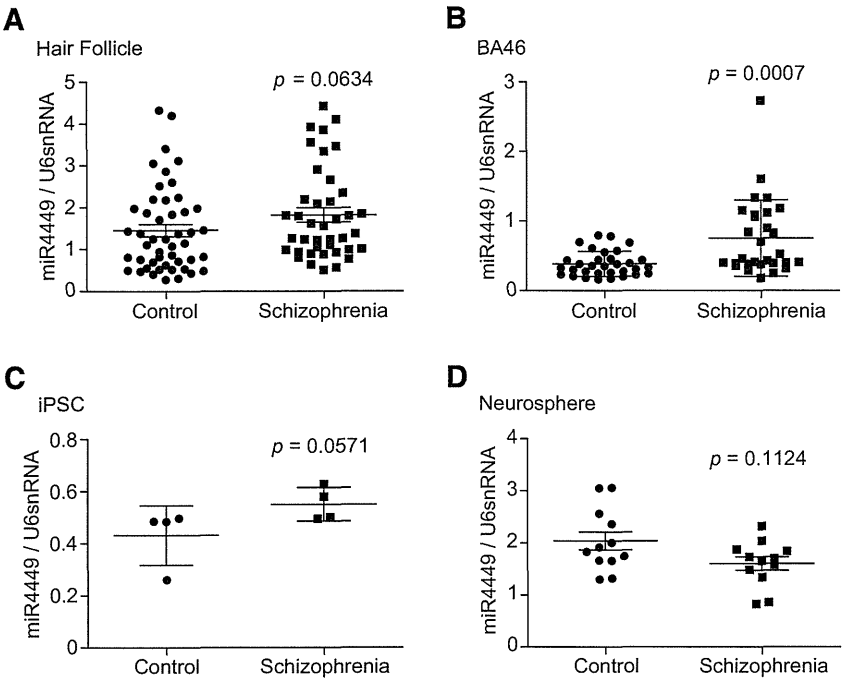

Figure 3. Expression analyses of *hsa-miR-4449* in schizophrenia and control samples. Results from hair follicles (the second sample set) **(A)**, postmortem brains (Brodmann area [BA]46) **(B)**, induced pluripotent stem cells (iPSCs) **(C)**, and neurospheres **(D)** are shown. U6 small nuclear RNA (snRNA) was used as an internal control. *p* values were calculated using two-tailed Mann-Whitney *U* test. Horizontal bars show mean ± SD.

genetic feature with the highest risk for schizophrenia, affecting around .3% of schizophrenia patients (32). The *FABP4* gene shows little expression in iPSCs derived from either control subjects or patients (data not shown). The gene is expressed in neurospheres, suggesting that its expression starts at a very early stage of neuronal development. Neurospheres are composed of free-floating clusters of neural stem or progenitor cells, differentiated from iPSCs. However, *FABP4* expression levels were not significantly different between control subjects and cases (Figure S6 in Supplement 1; expressional variance in the control group was large). Expression of *hsa-miR-4449* showed a trend of upregulation in iPSCs from patients (p = .0571) (Figure 3C); however, there was no differential expression between neurospheres derived from control subjects and cases (Figure 3D).

Examination of Autism Samples

We also performed a preliminary study to examine whether expression patterns of putative autism genes in scalp hair follicles could discriminate between autism and control samples. The sample cohort is shown in Table 1. We selected genes from candidates for autism susceptibility and included *FABP4*, due to the genetic overlap between schizophrenia and autism (33). The remaining genes were *FABP7* (9), *NHE6* (34), *NHE9* (34), *A2BP1* (35), *CADPS2* (36), *AH1* (35), *CNTNAP2* (35), and *SLC25A12* (35). Of the nine genes, only *CADPS2* (p = .0401) and *CNTNAP2* (p = .0212) showed significantly decreased expression in autism-derived samples compared with control follicles (Figure S7 in Supplement 1). It should be noted that the average age of autism subjects was significantly lower than that of control subjects (Table 1) and that *CADPS2* levels showed a positive correlation with age in autism and control + autism groups (Figure S8 in Supplement 1). Therefore, we can only safely nominate *CNTNAP2* level as a potentially valid marker for autism in this study (Figure S9 in Supplement 1). Approximately half of the examined patients were medicated. However, these patients were not outliers in terms of *CNTNAP2* expression in hair follicles; that is, they fell within the mean ± 2SD (detailed data not shown).

DISCUSSION

We examined and attempted to validate expression levels of schizophrenia and autism candidate genes using scalp hair follicles as a surrogate source of disease markers. Of the protein-coding genes tested that are putative schizophrenia genes, *FABP4* was confirmed to be downregulated in disease samples in our two-stage analyses. Our low rate of replication could be due to two main factors. First, the current sample size is insufficient, which may represent one of the limitations in this study. Another potential reason might be that stable detection of expression levels is dependent on where a particular gene is expressed in the hair follicle. For instance, *FABP4* is expressed in more central portions (IRS and cortex) of the hair follicle and the integrity of these areas may be well maintained during the plucking process, leading to more consistent results.

FABP4, also known as adipocyte-specific fatty acid-binding protein, belongs to the fatty acid-binding protein super family, whose members have molecular masses of approximately 15,000. FABPs are highly conserved cytoplasmic proteins that bind long-chain fatty acids and other hydrophobic ligands. It is thought that FABPs are active in fatty acid uptake, transport, and metabolism. In the periphery, FABP4 is highly expressed in adipose tissue and moderately expressed in macrophages, endothelial cells, and bone marrow (37). The protein has been intensively studied in terms of systemic insulin sensitivity and

A

Diagnosis	Sex	Age	Fibroblast	iPSC line No.
Control	F	36	B7	201B7, YA9
Control	F	16	WD	39
Control	M	40	KA	23
Schizophrenia with 22q11del	F	30	KO001	19, 25
Schizophrenia with 22q11del	F	37	SA001	1D2, 3B1

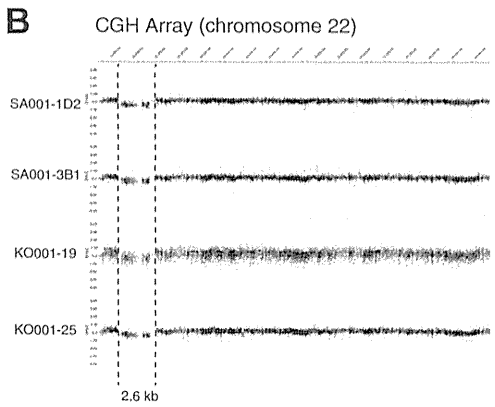

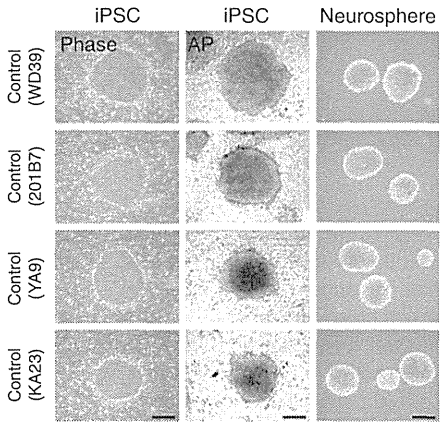

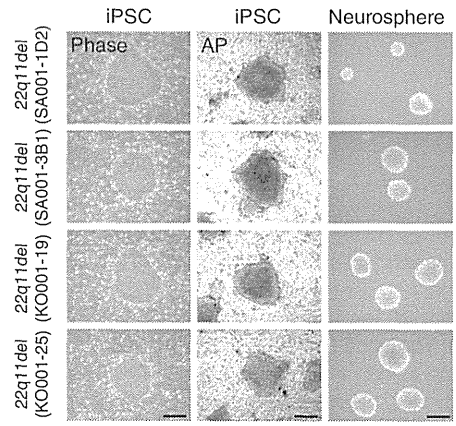

Figure 4. Establishment of iPSCs and iPSC-derived neurospheres from controls and schizophrenia patients with a 22q11.2 deletion (also see ref. 31). **(A)** Demographic data and I.D. information for samples are shown. **(B)** CGH array analysis of chromosome 22 using iPSCs showed that all the iPSC lines derived from the patients carried a 2.6 Mb hemizygous deletion at chromosome 22q11.2. **(C)** Alkaline phosphatase (AP) staining of iPSCs from controls (WD39, 201B7, YA9 and KA23). AP activity was detected using an Alkaline Phosphatase Staining kit (Miltenyi Biotec, Bergisch Gladbach, Germany). **(D)** Those from patients with a 22q11.2 deletion (SA001-1D2, SA001-3B1, KO001-19 and KO001-25). All the iPSC clones were AP-positive showing the pluripotency. Scale bars: phase contrast and AP staining, 400 μm; neurospheres, 150 μm. iPSC, induced pluripotent stem cells.

lipid and glucose metabolism, both of which correlate with inflammatory mechanisms (21). Since the results showing downregulation of *FABP4* in scalp hair follicles from schizophrenia subjects are robust against confounding factors, including those related to metabolic state, our findings are unlikely to represent either metabolic or inflammatory conditions. In addition, our patients had been treated with second-generation antipsychotics, including olanzapine, which often induce metabolic syndrome, but *FABP4* levels in hair follicles were independent of drug dose and duration of illness. Conformingly, there was no significant correlation between serum FABP4 and *FABP4* transcript levels in hair follicles. Therefore, elevated *FABP4* expression in hair follicles may point toward a pathophysiological step in schizophrenia.

In our protocol, all cells in neurospheres expressed the neural markers Nestin, or β3-tubulin, suggesting that our neurospheres consist almost entirely of neural stem or progenitor cells (38). The fact that *FABP4* is expressed in neurospheres may suggest a potential role in neuronal stem cell maintenance or neuronal differentiation or both processes. Although iPSC-derived neurospheres showed no significant differences in *FABP4* expression levels between control and schizophrenia cohorts, before a conclusion can be made, it would be necessary to examine a much larger cohort. According to the Human Protein Atlas database (Knut and Alice Wallenberg Foundation, Stockholm, Sweden; http://www.proteinatlas.org/), *FABP4* transcripts are expressed in neuronal cells (35%) and glial and endothelial cells (65%) of the adult cerebral cortex.

To evaluate whether common genetic variants of *FABP4* determine a predisposition to schizophrenia, we performed a genetic association study using approximately 2000 schizophrenia cases and 2000 age- and sex-matched control subjects with six tag single nucleotide polymorphisms (Supplementary Methods and Materials in Supplement 1). This analysis found no significant allelic or genotypic association (Table S4 in Supplement 1). The *FABP4* gene is composed of two haplotype blocks, based on Gabriel's confidence intervals (39) (Figure S10 in Supplement 1). Haplotype analysis also failed to reveal any significant signals. The exact reasons for the different directional changes seen in hair follicles, serum, postmortem brains, and neurospheres between control and schizophrenia subjects remain unknown. All *FABP* family genes contain a canonical TATA box, followed by a conserved gene structure. The tissue-specific and developmental regulation of *FABP* subtype expression, including that of *FABP4*, is thought to be controlled by unidentified genomic regulatory elements (6,40).

Mechanistically speaking, although not yet confirmed, the *FABP4* may be more central to schizophrenia pathophysiology beyond being a mere biomarker for disease. This is based on the following observations: 1) *FABP4* is expressed in the early neuronal lineage (a current finding); 2) other *FABP* genes are

reported to be associated with schizophrenia (6,7,9,11); and 3) there is evidence linking polyunsaturated fatty acids (endogenous ligands for FABPs) with schizophrenia etiology (41) and brain development (42).

Regarding miRNA, we detected *hsa-miR-4449* from a total of 1919 human mature miRNAs in this study. Although its expression in hair follicles was not significantly altered, expression did show significant upregulation in postmortem brains (BA46) and a trend of increase in iPSCs from schizophrenia samples. Web-based target predictions for *hsa-miR-4449* hit 18 protein-coding genes using TargetScan (Whitehead Institute for Biomedical Research, Release 6.2) (Table S5 in Supplement 1) and 10 protein-coding genes using miRDB (Washington University School of Medicine; http://mirdb.org/miRDB/) (Table S6 in Supplement 1). Between the two programs, the following three genes overlapped: 1) *HIC1*; 2) *RBM4*; and 3) *TOMM40*. Although the predicted roles for these three genes in schizophrenia pathogenesis are not known, *hsa-miR-4449* would make an interesting candidate in future studies, since this miRNA is expressed in early human neurodevelopmental stages such as iPSCs and iPSC-derived neurospheres.

In the analysis of autism-derived scalp hair follicles, we found significant downregulation of *CNTNAP2* in sufferers compared with control subjects and that the results are not affected by age. *CNTNAP2*, which encodes the contactin associated protein-like 2, is one of the strongest autism susceptibility genes with convergent evidence from several independent studies (43).

In the case of schizophrenia, biomarkers are an essential tool, particularly in the early phase of disease onset, such as the prodromal phase or at-risk mental state (44). It would be important to confirm whether *FABP4* expression levels in scalp hair follicles constitute a valid measure for discriminating between those individuals in at-risk mental state who will spontaneously recover and those who will need therapeutic treatment. As a starting point, it is interesting that the decreased *FABP4* levels in schizophrenia-derived hair follicles are not influenced by duration of illness.

In summary, our results provide an original concept for identifying novel disease markers, with potential benefits for the clinical practice of psychiatric medicine, as well as possible applications to other brain disorders. The development of methods that enable the analysis of a transcriptome using hair follicles (~10 samples) would be highly desirable. At the moment, approximately 40 ng of total RNA is extractable from a single hair follicle, but this amount is not enough for currently available cDNA microarray analysis, a technique which needs roughly 1 μg of total RNA.

ACKNOWLEDGMENTS AND DISCLOSURES

This study was supported, in part, by grants-in-aid for Scientific Research and by grant-in-aid for Scientific Research on Innovative Areas from the Japan Society for the Promotion of Science, Japan. In addition, this study was supported by RIKEN Brain Science Institute Funds, and a part of this study is the result of the "Development of biomarker candidates for social behavior" and "Integrated research on neuropsychiatric disorders" projects, carried out under the Strategic Research Program for Brain Sciences by the Ministry of Education, Culture, Sports, Science and Technology of Japan.

We thank Dr. Tomoe Ichikawa, Dr. Kazuya Toriumi, and Ms. Akiko Kobori at Department of Psychiatry and Behavioral Sciences, Tokyo Metropolitan Institute of Medical Science, for their help with collecting scalp hair follicle samples. We also thank Drs. Kenji J. Tsuchiya and Kaori Matsumoto at Research Center for Child Mental Development, Hamamatsu University School of Medicine, who have an established reliability of diagnosing autism with the Japanese version of Autism Diagnostic Interview-Revised and conducted the diagnostic tool.

The authors report no biomedical financial interests or potential conflicts of interest.

ARTICLE INFORMATION

From the Laboratory of Molecular Psychiatry (MMa, KY, MT, TO, YIway, CS, TT, YN, SB, TY), RIKEN Brain Science Institute, Saitama; Graduate School of Humanities and Sciences (CS), Department of Life Science, Ochanomizu University, Tokyo; Research Center for Child Mental Development (HM), University of Fukui, Fukui; Department of Psychiatry and Neurology (YIway, KS, NM), Hamamatsu University School of Medicine, Shizuoka; Department of Psychiatry and Behavioral Sciences (MMi, MI), Tokyo Metropolitan Institute of Medical Science, Tokyo; Department of Psychiatry and Neurobiology (MKi), Kanazawa University Graduate School of Medicine, Kanazawa; Department of Neuropsychiatry (MKi), Keio University School of Medicine, Tokyo; Physiology (YOk, WA, HO), Keio University School of Medicine, Tokyo; Department of Neurology (YOk), School of Medicine, Aichi Medical University, Aichi; Center for Genomic and Regenerative Medicine (WA), Juntendo University School of Medicine, Tokyo; and Department of Organ Anatomy (YOw), Yamaguchi University Graduate School of Medicine, Ube, Japan.

Address correspondence to Takeo Yoshikawa, M.D., Ph.D., Laboratory for Molecular Psychiatry, RIKEN Brain Science Institute, 2-1 Hirosawa, Wako, Saitama 351-0198, Japan; E-mail: takeo@brain.riken.jp.

Received Mar 17, 2014; revised Jul 24, 2014; accepted Jul 25, 2014.

Supplementary material cited in this article is available online at http://dx.doi.org/10.1016/j.biopsych.2014.07.025.

REFERENCES

1. Hashimoto T, Bazmi HH, Mirnics K, Wu Q, Sampson AR, Lewis DA (2008): Conserved regional patterns of GABA-related transcript expression in the neocortex of subjects with schizophrenia. Am J Psychiatry 165:479–489.
2. Benes FM, Berretta S (2001): GABAergic interneurons: Implications for understanding schizophrenia and bipolar disorder. Neuropsychopharmacology 25:1–27.
3. Tkachev D, Mimmack ML, Ryan MM, Wayland M, Freeman T, Jones PB, *et al.* (2003): Oligodendrocyte dysfunction in schizophrenia and bipolar disorder. Lancet 362:798–805.
4. Hakak Y, Walker JR, Li C, Wong WH, Davis KL, Buxbaum JD, *et al.* (2001): Genome-wide expression analysis reveals dysregulation of myelination-related genes in chronic schizophrenia. Proc Natl Acad Sci U S A 98:4746–4751.

5. Jitoku D, Hattori E, Iwayama Y, Yamada K, Toyota T, Kikuchi M, *et al.* (2011): Association study of Nogo-related genes with schizophrenia in a Japanese case-control sample. Am J Med Genet B Neuropsychiatr Genet 156B:581–592.
6. Watanabe A, Toyota T, Owada Y, Hayashi T, Iwayama Y, Matsumata M, *et al.* (2007): Fabp7 maps to a quantitative trait locus for a schizophrenia endophenotype. PLoS Biol 5:e297.
7. Iwayama Y, Hattori E, Maekawa M, Yamada K, Toyota T, Ohnishi T, *et al.* (2010): Association analyses between brain-expressed fatty-acid binding protein (FABP) genes and schizophrenia and bipolar disorder. Am J Med Genet B Neuropsychiatr Genet 153B:484–493.
8. Maekawa M, Takashima N, Matsumata M, Ikegami S, Kontani M, Hara Y, *et al.* (2009): Arachidonic acid drives postnatal neurogenesis and elicits a beneficial effect on prepulse inhibition, a biological trait of psychiatric illnesses. PLoS One 4:e5085.
9. Maekawa M, Iwayama Y, Arai R, Nakamura K, Ohnishi T, Toyota T, *et al.* (2010): Polymorphism screening of brain-expressed FABP7, 5 and 3 genes and association studies in autism and schizophrenia in Japanese subjects. J Hum Genet 55:127–130.
10. Freeman MP, Hibbeln JR, Wisner KL, Davis JM, Mischoulon D, Peet M, *et al.* (2006): Omega-3 fatty acids: Evidence basis for treatment and future research in psychiatry. J Clin Psychiatry 67:1954–1967.
11. Shimamoto C, Ohnishi T, Maekawa M, Watanabe A, Ohba H, Arai R, *et al.* (2014): Functional characterization of FABP3, 5 and 7 gene variants identified in schizophrenia and autism spectrum disorder and mouse behavioral studies [published online ahead of print July 15]. Hum Mol Genet.
12. Lord C, Risi S, Lambrecht L, Cook EH Jr, Leventhal BL, DiLavore PC, *et al.* (2000): The autism diagnostic observation schedule-generic: A standard measure of social and communication deficits associated with the spectrum of autism. J Autism Dev Disord 30:205–223.
13. Suzuki K, Sugihara G, Ouchi Y, Nakamura K, Futatsubashi M, Takebayashi K, *et al.* (2013): Microglial activation in young adults with autism spectrum disorder. JAMA Psychiatry 70:49–58.
14. Takahashi K, Tanabe K, Ohnuki M, Narita M, Ichisaka T, Tomoda K, Yamanaka S (2007): Induction of pluripotent stem cells from adult human fibroblasts by defined factors. Cell 131:861–872.
15. Imaizumi Y, Okada Y, Akamatsu W, Koike M, Kuzumaki N, Hayakawa H, *et al.* (2012): Mitochondrial dysfunction associated with increased oxidative stress and alpha-synuclein accumulation in PARK2 iPSC-derived neurons and postmortem brain tissue. Mol Brain 5:35.
16. Nori S, Okada Y, Yasuda A, Tsuji O, Takahashi Y, Kobayashi Y, *et al.* (2011): Grafted human-induced pluripotent stem-cell-derived neurospheres promote motor functional recovery after spinal cord injury in mice. Proc Natl Acad Sci U S A 108:16825–16830.
17. Yagi T, Ito D, Okada Y, Akamatsu W, Nihei Y, Yoshizaki T, *et al.* (2011): Modeling familial Alzheimer's disease with induced pluripotent stem cells. Hum Mol Genet 20:4530–4539.
18. Andreasen NC, Pressler M, Nopoulos P, Miller D, Ho BC (2010): Antipsychotic dose equivalents and dose-years: A standardized method for comparing exposure to different drugs. Biol Psychiatry 67:255–262.
19. Inagaki A, Inada T (2006): Dose equivalence of psychotropic drugs. Part 18: Dose equivalence of psychotropic drugs: 2006-version. Jpn J Clin Psychopharmacol 9:1443–1447.
20. Cao H, Sekiya M, Ertunc ME, Burak MF, Mayers JR, White A, *et al.* (2013): Adipocyte lipid chaperone AP2 is a secreted adipokine regulating hepatic glucose production. Cell Metab 17:768–778.
21. Kralisch S, Fasshauer M (2013): Adipocyte fatty acid binding protein: A novel adipokine involved in the pathogenesis of metabolic and vascular disease? Diabetologia 56:10–21.
22. Ishimura S, Furuhashi M, Watanabe Y, Hoshina K, Fuseya T, Mita T, *et al.* (2013): Circulating levels of fatty acid-binding protein family and metabolic phenotype in the general population. PLoS One 8: e81318.
23. Daly EJ, Kent JM, Janssens L, Newcomer JW, Husken G, De Boer P, *et al.* (2013): Metabolic and body mass parameters after treatment with JNJ-37822681, a novel fast-dissociating D2 receptor antagonist, vs olanzapine in patients with schizophrenia. Ann Clin Psychiatry 25: 173–183.
24. Hahn MK, Wolever TM, Arenovich T, Teo C, Giacca A, Powell V, *et al.* (2013): Acute effects of single-dose olanzapine on metabolic, endocrine, and inflammatory markers in healthy controls. J Clin Psychopharmacol 33:740–746.
25. Mistriotis P, Andreadis ST (2013): Hair follicle: A novel source of multipotent stem cells for tissue engineering and regenerative medicine. Tissue Eng Part B Rev 19:265–278.
26. Langbein L, Rogers MA, Praetzel-Wunder S, Helmke B, Schirmacher P, Schweizer J (2006): K25 (K25irs1), K26 (K25irs2), K27 (K25irs3), and K28 (K25irs4) represent the type I inner root sheath keratins of the human hair follicle. J Invest Dermatol 126:2377–2386.
27. Schweizer J, Bowden PE, Coulombe PA, Langbein L, Lane EB, Magin TM, *et al.* (2006): New consensus nomenclature for mammalian keratins. J Cell Biol 174:169–174.
28. Imaizumi Y, Okano H (2014): Modeling human neurological disorders with induced pluripotent stem cells. J Neurochem 129:388–399.
29. Okano H, Yamanaka S (2014): iPS cell technologies: Significance and applications to CNS regeneration and disease. Mol Brain 7:22.
30. Horiuchi Y, Kano S, Ishizuka K, Cascella NG, Ishii S, Talbot CC Jr, *et al.* (2013): Olfactory cells via nasal biopsy reflect the developing brain in gene expression profiles: Utility and limitation of the surrogate tissues in research for brain disorders. Neurosci Res 77:247–250.
31. Bundo M, Toyoshima M, Okada Y, Akamatsu W, Ueda J, Nemoto-Miyauchi T, *et al.* (2014): Increased l1 retrotransposition in the neuronal genome in schizophrenia. Neuron 81:306–313.
32. Rees E, Walters JT, Georgieva L, Isles AR, Chambert KD, Richards AL, *et al.* (2014): Analysis of copy number variations at 15 schizophrenia-associated loci. Br J Psychiatry 204:108–114.
33. Cross-Disorder Group of the Psychiatric Genomics Consortium, Lee SH, Ripke S, Neale BM, Faraone SV, Purcell SM, *et al.* (2013): Genetic relationship between five psychiatric disorders estimated from genome-wide SNPs. Nat Genet 45:984–994.
34. Schwede M, Garbett K, Mirnics K, Geschwind DH, Morrow EM (2014): Genes for endosomal NHE6 and NHE9 are misregulated in autism brains. Mol Psychiatry 19:277–279.
35. Voineagu I, Wang X, Johnston P, Lowe JK, Tian Y, Horvath S, *et al.* (2011): Transcriptomic analysis of autistic brain reveals convergent molecular pathology. Nature 474:380–384.
36. Sadakata T, Furuichi T (2009): Developmentally regulated Ca2+-dependent activator protein for secretion 2 (CAPS2) is involved in BDNF secretion and is associated with autism susceptibility. Cerebellum 8:312–322.
37. Boord JB, Fazio S, Linton MF (2002): Cytoplasmic fatty acid-binding proteins: Emerging roles in metabolism and atherosclerosis. Curr Opin Lipidol 13:141–147.
38. Matsui T, Takano M, Yoshida K, Ono S, Fujisaki C, Matsuzaki Y, *et al.* (2012): Neural stem cells directly differentiated from partially reprogrammed fibroblasts rapidly acquire gliogenic competency. Stem Cells 30:1109–1119.
39. Gabriel SB, Schaffner SF, Nguyen H, Moore JM, Roy J, Blumenstiel B, *et al.* (2002): The structure of haplotype blocks in the human genome. Science 296:2225–2229.
40. Haunerland NH, Spener F (2004): Fatty acid-binding proteins—insights from genetic manipulations. Prog Lipid Res 43:328–349.
41. Maekawa M, Owada Y, Yoshikawa T (2011): Role of polyunsaturated fatty acids and fatty acid binding protein in the pathogenesis of schizophrenia. Curr Pharm Des 17:168–175.
42. Basak S, Das MK, Duttaroy AK (2013): Fatty acid-induced angiogenesis in first trimester placental trophoblast cells: Possible roles of cellular fatty acid-binding proteins. Life Sci 93:755–762.
43. Penagarikano O, Geschwind DH (2012): What does CNTNAP2 reveal about autism spectrum disorder? Trends Mol Med 18:156–163.
44. Schultze-Lutter F, Schimmelmann BG, Ruhrmann S (2011): The near Babylonian speech confusion in early detection of psychosis. Schizophr Bull 37:653–655.

Krajarng et al. BMC Complementary and Alternative Medicine (2015) 15:26
DOI 10.1186/s12906-015-0544-4

BMC Complementary & Alternative Medicine

RESEARCH ARTICLE Open Access

Apoptosis induction associated with the ER stress response through up-regulation of JNK in HeLa cells by gambogic acid

Aungkana Krajarng[1,2], Masaya Imoto[3], Etsu Tashiro[3], Takahiro Fujimaki[3], Satoko Shinjo[3] and Ramida Watanapokasin[2*]

Abstract

Background: Gambogic acid (GA) was extracted from the dried yellow resin of gamboge (*Garcinia hanburyi*) which is traditionally used as a coloring material for painting and cloth dying. Gamboge has been also used as a folk medicine for an internal purgative and externally infected wound. We focused on the mechanisms of apoptosis induction by GA through the unfold protein response (ER stress) in HeLa cells.

Methods: The cytotoxic effect of GA against HeLa cells was determined by trypan blue exclusion assay. Markers of ER stress such as XBP-1, GRP78, CHOP, GADD34 and ERdj4 were analyzed by RT-PCR and Real-time RT-PCR. Cell morphological changes and apoptotic proteins were performed by Hoechst33342 staining and Western blotting technique.

Results: Our results indicated a time- and dose-dependent decrease of cell viability by GA. The ER stress induction is determined by the up-regulation of spliced XBP1 mRNA and activated GRP78, CHOP, GADD34 and ERdj4 expression. GA also induced cell morphological changes such as nuclear condensation, membrane blebbing and apoptotic body in Hela cells. Apoptosis cell death detected by increased DR5, caspase-8, −9, and −3 expression as well as increased cleaved-PARP, while decreased Bcl-2 upon GA treatment. In addition, phosphorylated JNK was up-regulated but phosphorylated ERK was down-regulated after exposure to GA.

Conclusions: These results suggest that GA induce apoptosis associated with the ER stress response through up-regulation of p-JNK and down-regulation of p-ERK in HeLa cells.

Keywords: Gambogic acid, Anticancer, ER stress, Apoptosis, HeLa cells

Background

Gambogic acid (GA) is the major active ingredient of gamboge extracted from *Garcinia hanburyi* in Southeast Asia, India and China. It is commonly known in Thailand as "Rong Thong". It has been used as a folk medicine for an internal purgative and externally infected wound [1]. GA has potent anticancer effect, including induction of apoptosis and cell cycle arrest in a broad range of human cancer such as gastric cancer [2], leukemia [3], breast cancer [4] and hepatoma cancer [5]. It has been demonstrated that GA activates cell apoptosis through transferrin receptor [6] and nuclear factor-κB signaling pathway [7]. Previous study also showed that GA has anti-metastasis activity by suppressing the expression of integrin β1 [8]. Moreover, GA could inhibit tumor angiogenesis by decreasing VEGF production [9] and suppressing VEGFR2 [10]. Recently, Zhang et al. [11] showed that GA could be an inhibitor of Heat shock protein 90 (Hsp90) which is a key protein in cell signaling and tumor regeneration. Inhibition of Hsp90 by treatments of cells with specific inhibitors leads to ER stress induction and subsequent activation of the three ER stress sensors of the unfolded protein response which contributed to cell death of the treated cells [12].

The endoplasmic reticulum (ER) is a central organelle involved in lipid synthesis, protein folding and

* Correspondence: ramida.swu@gmail.com
[2]Department of Biochemistry, Faculty of Medicine, Srinakharinwirot University, Bangkok, Thailand
Full list of author information is available at the end of the article

maturation. The ER is highly sensitive to stress that disturb cellular energy levels, the redox state or Ca^{2+} concentration. These reduce the protein folding capacity of the ER and cause the accumulation and aggregation of unfolded protein which result in ER stress response termed unfolded protein response (UPR). The ER stress response is regulated by three ER transmembrane receptors; pancreatic ER kinase (PKR)-like ER kinase (PERK), inositol requiring enzyme 1 (IRE1) and activating transcription factor 6 (ATF6) [13]. These ER transmembrane proteins are kept in an inactive state through their association with the ER chaperone BiP/GRP78 (glucose-related protein, 78kD). During ER stress, GRP78 dissociates from these three transmembrane proteins. Activated PERK blocks general protein synthesis by phosphorylating eukaryotic initiation factor 2 (eIF2α). This phosphorylation enables translation of ATF4 which translocates to the nucleus and induces the transcription of genes required to restore ER homeostasis. Activation of IRE1 by ER stress is typical of receptor kinase proteins, which homodimerize and transphosphorylate [14]. IRE1 splices X-box protein 1 (XBP1) mRNA to form mature XBP1s mRNA (s for spliced) which leads to not only the transcriptional activation of ER-associated protein degradation (ERAD) component genes and ER/Golgi biogenesis but also genes involved in redox homeostasis and oxidative stress response [15,16]. After the dissociation of GRP78, ATF6 translocates to the Golgi apparatus where it is cleaved into its active form by site-1 and site-2 protease. Active ATF6 then binds to ER stress response element (ERSE) in the nucleus to activate transcription of ER chaperone genes such as GRP78, GRP94, and the transcription factors C/EBP homologous protein (CHOP) and XBP1 [17]. ER stress has recently been identified as another major pathway engaged in the initiation of apoptosis [18]. Severe or prolonged ER stress stimulates PERK, ATF6 and IRE1 apoptotic signaling and increase CHOP expression. It has been showed that CHOP is a critical ER stress-induced apoptosis molecule through regulating the expression of Bcl2, Bim and DR5 [19,20].

Cervical cancer is the fourth most common cancer in woman worldwide and it remains a leading cause of death from cancer in developing and low income countries [21]. In this study, we have shown for the first time that GA can induce apoptosis in cervical cancer HeLa cells associated with the ER stress response by up-regulation of CHOP, p-JNK and down-regulation of p-ERK.

Methods

Preparation of gambogic acid (GA)

Garcinia hanburyi was collected from Laem-ngob, Trat province, Thailand in Jan 2012. A voucher specimen (Montree Kurukitkoson No. 001) was deposited at the Faculty of Medicine, Srinakharinwirot University, Bangkok, Thailand. GA (Figure 1A) was isolated from gamboge (*G. Hanburyi*). The extraction and separation method was as followed: dried resin of gamboge (1 g) was grounded into a powder and extracted with acetone: dH_20 (1:1, 1 L), followed by ethyl acetate (1:1). After evaporation, the extract yielded as a yellowish solid (0.6 g). A portion of extract (0.3 g) was subjected to silica gel column chromatography (Silica gel 60, 60–230 μm, Merck, Darmstadt, Germany) using chloroform/methanol stepwise system and yielded the major compound, GA, including other minor compounds. Repeated purification of these column fractions was performed on a SSC-1311 recycling HPLC system equipped with a SSC-5410 UV–vis detector and SSC-3462 pump (Senshu Scientific, Japan). The column was Capcell Pak C18, type UG80 (20 mm id. × 250 mm, 5 μm, Shiseido, Japan). The mobile phase was 75% acetonitrile at a flow rate of 10 ml/min. The UV detection wavelength was set at 360 nm. The chemical structures of GA were then identified by comparing their ^{1}H NMR and ^{13}C NMR spectra (JNM-ECA500 NMR, JEOL, Japan) with the literature data [22]. GA was dissolved and diluted in methanol (Wako, Japan) at the desired concentration for assays.

Cell culture

Human cervical carcinoma HeLa cells were obtained from the American Type Culture Collection (ATCC, Manassas, VA). Cells were cultured in Dulbecco's modified Eagle's medium (Nissui, Tokyo, Japan) containing 8% fetal bovine serum, 2.5 g/L sodium bicarbonate, and penicillin G (100 units/mL).The medium was refreshed every 2–3 days. After about 70% confluence, the cultured cells were detached with 0.25% trypsin-EDTA and sub-cultured.

Cell viability

The effect of GA on cell viability was analyzed by using trypan blue exclusion method. Cells were seeded in a 48-well plate at 1×10^4 cells/well and incubated overnight. Then, the cells were treated with the indicated concentrations (0, 0.03, 0.1, 0.3, 1, 3 μg/mL) of GA for 4, 8, 12, 16, 20 and 24 h. The control cells were treated with the solvent (methanol) used to prepare the GA. Cells were trypsinized and stained with trypan blue then counted with a hemocytometer. Cell survival was expressed as percentage of viable cells to total cells. Cells were treated in triplicate, and the experiments were repeated three times.

RT-PCR analysis

HeLa cells were seeded in a 12-well plate at 5×10^4 cells/well for overnight. Then cells were treated with

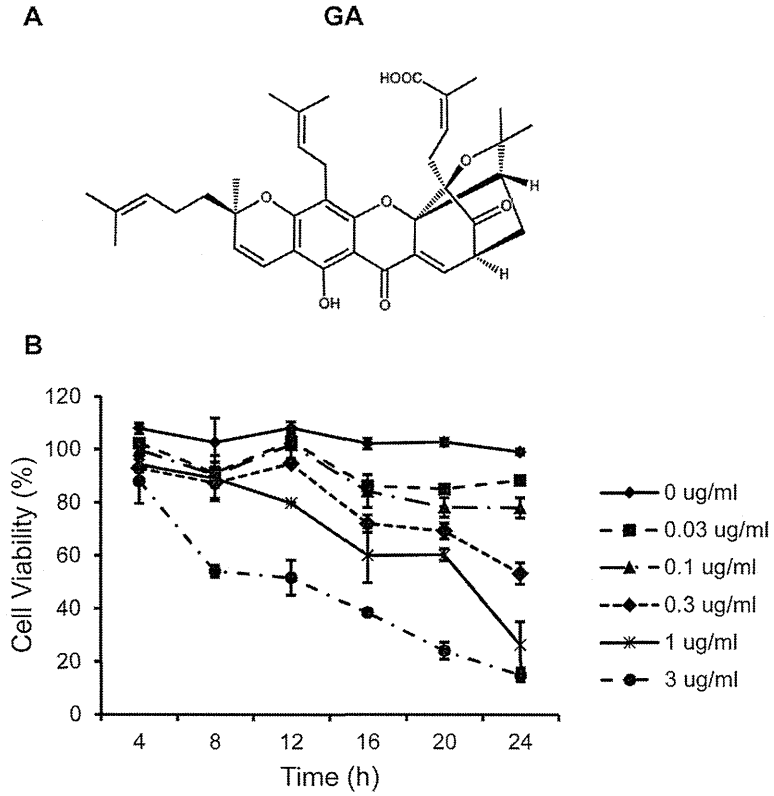

Figure 1 GA inhibits cell growth in HeLa cells. (A) Formula of Gambogic acid (GA). **(B)** Effect of GA on cell viability in HeLa cells. Time- and dose-dependent effect of GA was performed when HeLa cells were treated with various concentrations of GA at different time points and their viability was determined by trypan blue exclusion assay. Results are mean values ± SD of three independent experiments (n = 3).

0.3 μg/mL of GA, 10 μg/mL tunicamycin as a positive control, for 4 and 8 h. Then total RNA from HeLa cells was extracted by using TRIzol reagent (Invitrogen, Carlsbad, CA). The cDNA was reverse transcribed from 2 μg of total RNA with oligo (dT) and M-MLV reverse transcriptase (Promega, Madison, WI). PCR was carried out with KOD Plus polymerase (Toyobo, Osaka, Japan) using a pair of primers corresponding to nucleotides 505–525 (AATGAAGTGAGGCCAGTGGCC) and 609–629 (CCCATGGATTCTGGCGGTATT) of XBP1 cDNA. The amplified products were separated by electrophoresis on 8% polyacrylamide gel and visualized with ethidium bromide staining.

Real-time RT-PCR

For quantification, real-time PCR was performed with SYBR Premix Ex Taq (Takara, Siga, Japan). The primers used for amplification were as followed: GRP78, forward 5′-GCTCGACTCGAATTCCAAAG-3′ and reverse 5′-GATCACCAGAGAGCACACCA-3′; CHOP, forward 5′-GCGCATGAAGGAGAAAGAAC-3′ and reverse 5′-TCACCATTCGGTCAATCAGA-3′; ERdj4, forward 5′-AAAATAAGAGCCCGGATGCT-3′ and reverse 5′-CGC TTCTTGGATCCAGTGTT-3′; GADD34, forward 5′-AA ACCAGCAGTTCCCTTCCT-3′ and reverse 5′-CTCTT CCTCGGCTTTCTCCT-3′ and GAPDH, forward 5′-AG GTCGGAGTCAACGGATTT-3′ and reverse 5′-TAGTT GAGGTCAATGAAGGG-3′

Nuclear morphology staining with Hoechst 33342

HeLa cells (2×10^5 cells/well in a six-well plate) were treated with 0.3 μg/mL GA for 0, 8, 16 and 24 h. After trypsinization, cells were washed with 1X PBS and stained with 3 μg/ml of Hoechst 33342 (Molecular Probes, Invitrogen, USA) for 15 min. Stained cells were examined using fluorescence microscope (Olympus, Tokyo, Japan) with an ultraviolet filter.

Western blot analysis

HeLa cells were incubated for different times in the presence or absence of 0.3 μg/mL of GA, harvested and washed once with ice cold PBS. Then, 2×10^5 cells were lysed for 30 min on ice in 50 μl of RIPA lysis buffer (50 mM Tris–HCl, pH 7.5, 5 mM EDTA, 250 mM NaCl, 0.5% Triton X-100) containing complete mini protease inhibitor cocktail (Roche Diagnostics GmbH,

Mannheim, Germany). Clear cell lysate supernatants were prepared by centrifugation and the protein content was determined using Bio-Rad protein assay (Bio-Rad Laboratories, USA). Proteins were separated by 12% SDS-PAGE and transferred onto polyvinylidene fluoride (PVDF) membranes (Pall Corporation, USA) for 1 h at 100 V with the use of a Mini Trans-Blot Cell® (Bio-Rad). After blocking with TBST (10 mM Tris, pH 7.5, 150 mM NaCl and 0.1% Tween 20) containing 5% nonfat milk, the blots were incubated overnight at 4°C with primary antibody (Cell Signaling Technology, Beverly, MA.) The membranes were washed in TBST and the appropriate secondary antibody conjugated with horseradish peroxidase (Cell Signaling Technology, Beverly, MA) was added for 1 h at room temperature. Immunoreactive protein bands were detected by chemiluminescence using enhanced chemiluminescence reagent (ECL, Millipore, Bedford, MA). The membranes were stripped and reprobed with β-actin antibody to assess protein loading for each lane.

Statistical analysis

All values were represented as mean ± S.D. One way analysis variance (ANOVA) was used in multi comparisons between groups. Statistical significance is accepted at $p < 0.05$.

Results

GA decreases cell viability in HeLa cells

We first examined the effect of GA on the cell viability of HeLa cells. The cells were treated with various concentrations of GA (0–3 μg/ml) for 4, 8, 12, 16, 20, 24 h. The cell viability was then evaluated using trypan blue exclusion method. The result showed that GA decreased cell viability in a time- and dose-dependent manner (Figure 1B). GA concentration at 0.3 μg/ml was used for subsequent experiments.

GA induces ER stress induction in HeLa cells

In response to ER stress, IRE1 splices a 26 nucleotide long intron of inactive unspliced XBP1 mRNA (XBP1u), generating an active and stable transcription factor XBP1s. To access whether GA triggers ER stress, we analyzed XBP1 mRNA splicing in HeLa cells. The XBP1 cDNA was amplified by RT-PCR. Tunicamycin (Tm), a well-recognized inducer of ER stress, served as a positive control in these tests. The result showed GA induced XBP1 splicing at 4 h and the XBP1 mRNA was elevated by approximately 6 fold compared to the level observed in control cells (0 h) (Figure 2). In contrast to Tm, the expression of XBP1 splicing was decreased following treatment with GA for 4 h to 8 h.

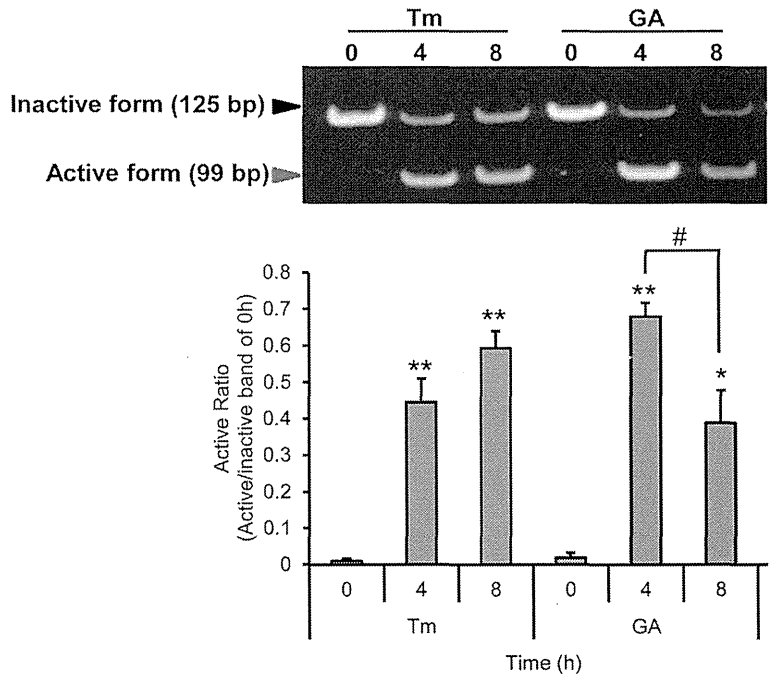

Figure 2 GA induces XBP1 mRNA splicing in HeLa cells. HeLa cells were treated with 10 μg/ml of tunicamycin (Tm) or 0.3 μg/ml of GA for 0, 4 and 8 h. mRNA was extracted and subjected to the RT-PCR. The active form was normalized to the inactive form at 0 h. Results are mean values ± SD of three independent experiments (n = 3). *$p < 0.05$; **$p < 0.01$ shows significant difference compared with 0 h; #$p < 0.05$, is significantly different as compared between 4 h and 8 h.

We further examined whether GA induced ER stress. The mRNA expression levels of ER stress-associated molecules (GRP78, CHOP, endoplasmic reticulum-localized DnaJ homologues (ERdj4) and growth arrest and DNA damage-inducible protein (GADD34)) were investigated by real -time PCR. CHOP, also known as GADD153, encodes a member of the CCAAT/enhancer-binding protein family and acts as an inhibitor or activator of transcription, leading to apoptosis [20]. ERdj4, which is a chaperone protein localized in the ER, is a downstream gene of XBP1, while GADD34 is downstream gene of eIF2α. Figure 3 showed GRP78 was slightly increased at 8 h in cells treated with GA. On the other hand, Tm showed obviously increased GRP78 expression and the highest level at 8 h. In addition, there was a large increase in CHOP and ERdj4 level between 4 and 8 h following exposure to Tm and GA. It is noticed that GA increased GADD34 expression, while it had very little effect in cells treated with Tm. All of these observations strongly imply that GA induced ER stress in HeLa cells.

GA induce apoptosis through intrinsic and extrinsic pathways in HeLa cells

To observe the morphological effects of HeLa cells in a time-dependent incubation of GA, cells were stained with Hoechst33342 and examined under a bright-field and fluorescence microscope. It showed that GA-treated cells which had nuclear condensation, membrane blebbing, shrunken and became apoptotic body in a time-dependent manner, while the control cells were of round shapes (Figure 4). This result indicated that the morphological changes of HeLa cells by GA were due to apoptosis.

To examine whether GA can induce apoptosis in HeLa cells, we examined the activation of caspases and Poly (ADP-ribose) polymerase (PARP), a substrate of caspase 3, by Western blotting. As shown in Figure 5A, GA reduced procaspase-8, −9 and −3 protein levels and increased active cleaved caspase-8, −9 and −3 and PARP cleavage. These results demonstrate that GA is involved in apoptosis induction in HeLa cells.

ER stress-induced apoptosis occurs in both intrinsic and extrinsic apoptosis pathways. Bcl-2 family of proteins such as Bcl-2, Bax and Bim are involved in regulating the intrinsic or mitochondrial apoptotic pathway. Western blotting results revealed the decreased Bcl-2 level in GA-treated cells in a time-dependent manner (Figure 5B). No significant change in Bax level was observed upon GA treatment. Previous study reported that Bim, a pro-apoptotic BH3-only member of the Bcl-2 family, is essential for ER stress-induced apoptosis [23].

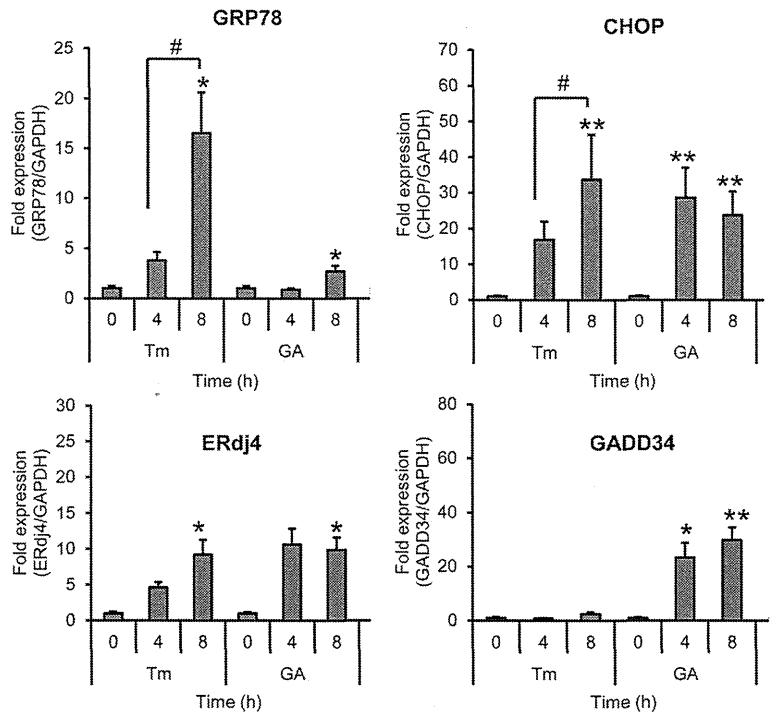

Figure 3 GA induces ER stress via up-regulation of GRP78, CHOP, ERdj4 and GADD34 mRNA. HeLa cells were treated with 10 μg/ml of tunicamycin (Tm) or 0.3 μg/ml of GA for 0, 4 and 8 h. Cells were collected and mRNA was extracted and evaluated by real-time RT-PCR. Each mRNA was normalized with the mRNA of GAPDH. Data are the results of three independent experiments, expressed as the mean ± SD, n = 3. *$p < 0.05$; **$p < 0.01$ shows significant difference compared with 0 h; #$p < 0.05$, is significantly different as compared between 4 h and 8 h.

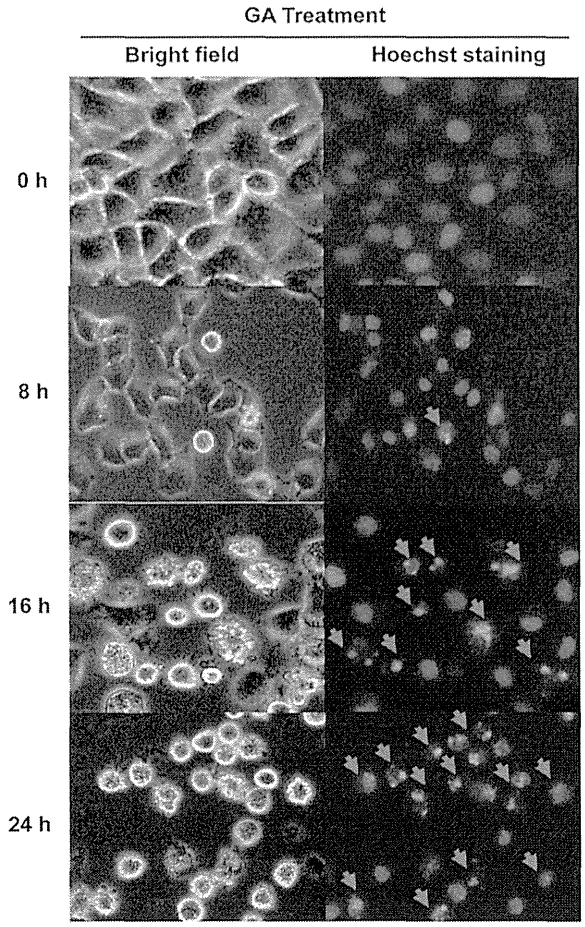

Figure 4 Effect of GA on cell morphological changes. HeLa cells were treated with 0.3 μg/ml of GA for 0, 8, 16 and 24 h. Cells were stained with Hoechst33342 and examined under a bright-field and fluorescence microscope (40X magnification). The arrows show cell morphological changes of apoptotic cells.

In this study, GA increased Bim in a time-dependent manner. These results demonstrate that the mitochondrial pathway is involved in GA-induced apoptosis in HeLa cell.

DR5 expression can be regulated at the transcriptional level through CHOP via binding to the CHOP-binding site in the DR5 gene 5′-flanking region [20]. DR5 also activates the downstream caspase-8 and the extrinsic apoptotic pathway [24]. The result showed DR5 protein level was increased in a time-dependent manner following GA treatment (Figure 5C). Our data suggest that DR5-mediated extrinsic apoptotic pathway is involved in GA-induced HeLa cell death.

Effect of GA on MAPK pathway

MAPKs are important signaling members of serine/threonine protein kinase family that control cellular proliferation, differentiation, survival and apoptosis. Three major mammalian MAPK subfamilies, extracellular regulated protein kinase (ERK), c-Jun N-terminal kinase (JNK) and p38, were activated through a specific phosphorylation cascade. In HeLa cells, GA decreased the level of phosphorylated ERK1/2 but not the total form (Figure 6). On the other hand, GA increased the level of phosphorylated JNK but decreased the level of total JNK protein after treatment with the compounds. In addition, GA did not affect p38 activity. The results suggested that GA may induce ER stress and apoptosis through the ERK and JNK MAPK pathways.

Discussion

GA, the major active compound extracted from gamboge, has been shown to induce apoptosis and inhibit cell growth in several cancer cell lines. However, this is the first study showing that ER stress is involved in GA-induced apoptosis in HeLa cells through up-regulaion of CHOP and p-JNK. Our study shows that GA can inhibit proliferation of HeLa cells in a dose- and time-dependent manner. GA concentration at 0.3 μg/ml was used for subsequent experiments because it showed the best results of ER stress but did not induce cell death at 4–8 h.

ER plays an important role in the maintenance of intracellular calcium homeostasis, protein synthesis, posttranslational modifications and protein folding. Recently, the potential of ER stress in tumor is considered important for regulating the balance between tumor cell death and growth, and for developing the sensitivity of chemotherapeutic agents [25]. ER stress is regulated by transmembrane proteins; PERK, IRE1 and ATF6. All of the three transmembrane proteins are activated through dissociation with GRP78 when there is an imbalanced of unfolded proteins and chaperones. The activation of IRE1 promotes XBP1 splicing. Spliced XBP1 is an active transcription factor that regulates the transcription of many target genes including ER chaperones and genes encoding the components of ER-associated degradation, such as ERdj4. Upon removal of GRP78, PERK autophosphorylates and activates in ER membrane. Activated PERK phosphorylates and inactivates eIF2α leads to the translational up-regulation of specific mRNAs, such as ATF4. ATF4 is a transcription factor that activates the transcription of pro-apoptotic factors CHOP and GADD34. Release of GRP78 frees ATF6 to translocate to the Golgi apparatus where resident proteases cleave ATF6, releasing this transcription factor into the cytosol and allowing it to migrate into the nucleus and regulate the gene expression [26].

The mechanisms underlying GA-induced ER stress are unknown. In this study, it showed GA could induce XBP1 splicing. However, it is notable that in response to the treatment with tunicamycin the active:inactive XBP1

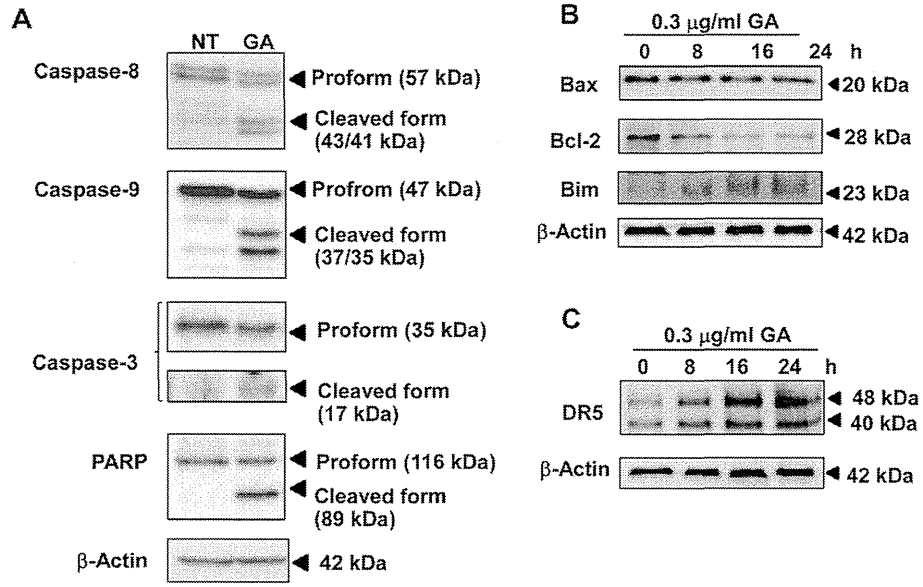

Figure 5 GA induces apoptosis. (A) The expression of caspase-3, −8, −9, and PARP were analyzed by Western blotting. HeLa cells were non treated (NT) or treated with 0.3 μg/ml of GA for 24 h. Effect of GA on the expression of **(B)** Bcl-2 family and **(C)** DR5 in HeLa cells. HeLa cells were treated with 0.3 μg/ml of GA for the indicated time points and analyzed by Western blotting. The results from representative experiments were expressed relative to the protein level at 0 h after normalization to β-actin signals.

ratio increased, while in response to the treatment of GA the ratio decreased after 8 h. This was due to cell death induction by GA, resulting in decreased active: inactive XBP1ratio, while tunicamycin did not. Furthermore, GA upregulated the mRNA levels of ER stress-associated molecules, including GRP78, CHOP, ERdj4 and GADD34. GADD34 is a target gene of the UPR and its induction in the early stress response promotes subsequent dephospholylation of eIF2α [27]. Tunicamycin is a typical inducer of ER stress that induces XBP1 splicing and activation of IRE1 [28]. Interestingly, GADD34 expression induced by GA was high, while it was not induced by tunicamycin. This finding suggests that GA induce ER stress in HeLa cells with different mechanism from that observed for tunicamycin. The modulation in the status of GRP-78 differs in response to the treatment with TM and GA could be explained according to Shinjo et al. [29]. The expression patterns of nine UTP target genes induced by seven UTP-inducing compounds including tunicamycin in HeLa cells were reported. These compounds were classified by hierarchical clustering analysis into two clusters; cluster A (thapsigargin, tunicamycin, 2-deoxyglucose, and dithiothreitol) and cluster B (brefeldin A, monensin, and eeyarestatin I). Their study also showed that the expression of GRP78 induced by brefeldin A is lower than by tunicamycin. Therefore, the difference in expression of UPR target gene profiles depends on the mode of action of compounds.

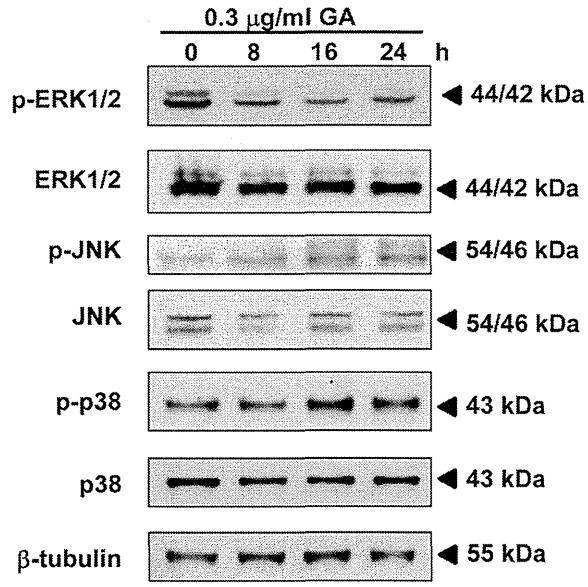

Figure 6 Effect of GA on MAPK pathway in HeLa cells. HeLa cells were treated with 0.3 μg/ml of GA for the indicated time points. The expression of phosphorylated and total ERK1/2, JNK and p38 were analyzed by Western blotting and were expressed relative to the protein level at 0 h after normalization to β-actin signals.

Furthermore, previous studies about ER stress in cancer showed that GRP78 promoted cancer cell proliferation, and not only protects cancer cells from the impact of microenvironment but also provides chemoresistance. Knockdown of GRP78 can suppress cancer cell growth and increase the sensitivity of cancer cells to

chemotherapeutic agents [30]. On the other hand, CHOP acts as an antagonist of GRP78 [31]. CHOP induces proapoptotic effect when ER stress is too severe to maintain cellular homeostasis. CHOP stimulates expression of GADD34 resulting in dephosphorylation of eIF2α and recovery of protein translation. High rates of protein synthesis during ER stress lead to cell death through the accumulation of misfolded proteins, which would reduce tumor mass. Then CHOP and GADD34 induce oxidative protein folding. Induction of GADD34 can contribute to chronic stress resulting in exaggerated toxicity and cell death. While suppression of CHOP and GADD34 promoted tumor growth, invasiveness and angiogenesis [32]. Therefore, GA showed little expression of GRP78 but high expression of CHOP and GADD34 may mediate tumor-suppressive effects.

Previous studies showed that GA could induce apoptosis in many cancer cells [2-5]. Liu et al. [33,34] reported that GA alone did not increase expression of CHOP and GRP78 but the combination of GA and calcium channel blocker verapamil or proteasome inhibitors bortezomib, induced high expression of these two proteins especially CHOP protein in human hepatoma HepG2 and leukemia K562 cells. Interestingly, GA alone did not induce apoptosis in both cell types but the combination of GA and verapamil or GA and bortezomib did, which is different from our results that only GA could induce ER stress and apoptosis in HeLa cells. Thus, these results show GA could induce different mechanism of ER stress and apoptosis pathways depending on cancer cell type.

This study also showed that GA induced apoptosis in HeLa cells via caspase-3, −8, −9 and PARP. ER stress can also activate well-known general regulators of apoptosis, including caspases and the Bcl-2 family of proteins. It has been known that Bcl-2 family members reside in the ER membrane and function principally at the mitochondrial outer membrane, so they may influence homeostasis and apoptosis from the ER as well [35,36]. Anti-apoptotic Bcl-2 or Bcl-X_L ,targeted specifically to the ER membrane, can block apoptosis induction by pharmacological kinase inhibition or by pro-apoptotic Bcl-2 family members. On the other hand, ER stress can activate several BH3-only pro-apoptotic members of the Bcl-2 family, including Bim, Bik, and Puma [37]. CHOP has been shown to promote apoptotic pathways, downstream of ER stress, by transcriptionally down-regulated the anti-apoptotic protein BCl-2 and up-regulate DR5, a member of the death receptor protein family [20]. We showed that GA could induce both intrinsic and extrinsic apoptotic pathways which involved in down-regulation of Bcl-2 protein, up-regulation of Bim protein as well as activation of caspase-8 and −9 and DR5.

In mammals, MAPKs guide cellular maturation and can induce inflammation and apoptosis. The MAPK family includes ERKs, which are activated by mitogens, and JNKs and p38 MAPKs that primarily activated by cytokines and in response to cellular stress [38]. It has been reported that ER stress caused the activation of JNK signaling pathway through IRE1-TRAF2 (TNF receptor associated factor 2) -ASK1 (Apoptosis signal-regulating kinase 1) pathway and up-regulated the pro-apoptotic activity of DR5, Puma, and Bim leading to apoptosis induction [39,40]. In this study, GA was shown to up-regulate phosphorylated JNK after 8 h of treatment. Furthermore, GA also showed down-regulated phosphorylated ERK but not p38. Our result suggests that GA induces apoptosis via up-regulation of JNK and down-regulation of ERK signaling pathway.

Conclusion

Although cell death mechanism during ER stress remains unclear, it seems that the death pathways depend both on the cancer type and on the tumor microenvironment. But in this study we have demonstrated for the first time that GA induces apoptosis associated with the ER stress response through up-regulation of JNK and down-regulation of ERK in HeLa cells. This finding suggests that GA could be a potential anticancer agent and these may offer further possibilities for alternative treatment.

Competing interests

The authors declare that they have no competing interests.

Authors' contributions

AK performed experiments and drafted the manuscript. MI and ET co-conceived the research theme, designed experiments. TF helped carrying out gambogic acid isolation and purification. SS helped with PCR, Western blotting and data analysis. RW is the principal investigator, initiated, co-conceived, coordinated the project and approve the final manuscript. All authors read and approved the final manuscript.

Acknowledgments

We would like to thank the Strategic Wisdom and Research Institute, Srinakharinwirot University, Bangkok, Thailand.

Author details

[1]Chulabhorn International College of Medicine, Thammasart University, Pratumthani, Thailand. [2]Department of Biochemistry, Faculty of Medicine, Srinakharinwirot University, Bangkok, Thailand. [3]Department of Biosciences and Informatics, Faculty of Science and Technology, Keio University, Yokohama, Japan.

Received: 23 March 2014 Accepted: 29 January 2015
Published online: 15 February 2015

References

1. Zhao L, Guo QL, You QD, Wu ZQ, Gu HY. Gambogic acid induces apoptosis and regulates expressions of Bax and Bcl-2 protein in human gastric carcinoma MGC-803 cells. Biol Pharm Bull. 2004;27(7):998–1003.
2. Liu W, Guo QL, You QD, Zhao L, Gu HY, Yuan ST. Anticancer effect and apoptosis induction of gambogic acid in human gastric cancer line BGC-823. World J Gastroenterol. 2005;11(24):3655–9.

3. Li R, Chen Y, Zeng L, Shu W, Zhao F, Wen L, et al. Gambogic acid induces G0/G1 arrest and apoptosis involving inhibition of SRC-3 and inactivation of Akt pathway in K562 leukemia cells. Toxicology. 2009;262(2):98–105.
4. Zhang HZ, Kasibhatla S, Wang Y, Herich J, Guastella J, Tseng B, et al. Discovery, characterization and SAR of gambogic acid as a potent apoptosis inducer by a HTS assay. Bioorg Med Chem. 2004;12(2):309–17.
5. Nie F, Zhang X, Qia Q, Yang L, Yang Y, Liu W, et al. Reactive oxygen species accumulation contributes to gambogic acid-induced apoptosis in human hepatoma SMMC-7721 cells. Toxicology. 2009;260(1–3):60–7.
6. Kasibhatla S, Jessen KA, Maliartchouk S, Wang JY, English NM, Drewe J, et al. A role for transferrin receptor in triggering apoptosis when targeted with gambogic acid. Proc Natl Acad Sci U S A. 2005;102(34):12095–100.
7. Pandey MK, Sung B, Ahn KS, Kunnumakkara AB, Chaturvedi MM, Aggarwal BB. Gambogic acid, a novel ligand for transferrin receptor, potentiates TNF-induced apoptosis through modulation of the nuclear factor-κB signaling pathway. Blood. 2007;110(10):3517–25.
8. Li C, Lu N, Qi Q, Li F, Ling Y, Chen Y, et al. Gambogic acid inhibits tumor cell adhesion by suppressing integrin β1 and membrane lipid rafts-associated integrin signaling pathway. Biochem Pharmacol. 2011;82(12):1873–83.
9. Lu N, Yang Y, You QD, Ling Y, Gao Y, Gu HY, et al. Gambogic acid inhibits angiogenesis through suppressing vascular endothelial growth factor-induced tyrosine phosphorylation of KDR/Flk-1. Cancer Lett. 2007;258(1):80–9.
10. Yi T, Yi Z, Cho SG, Luo J, Pandey MK, Aggarwal BB, et al. Gambogic acid inhibits angiogenesis and prostate tumor growth by suppressing vascular endothelial growth factor receptor 2 signaling. Cancer Res. 2008;68(6):1843–50.
11. Zhang L, Yi Y, Chen J, Sun Y, Guo Q, Zheng Z, et al. Gambogic acid inhibits Hsp90 and deregulates TNF-α/NF-αB in HeLa cells. Biochem Bioph Res Co. 2010;403(3–4):282–7.
12. Taiyab A, Sreedhar AS, Rao CM. Hsp90 inhibitors, GA and 17AAG, lead to ER stress-induced apoptosis in rat histiocytoma. Biochem Pharmacol. 2009;78(2):142–52.
13. Szegezdi E, Logue SE, Gorman AM, Samali A. Mediators of endoplasmic reticulum stress-induced apoptosis. EMBO Rep. 2006;7(9):880–5.
14. Shamu CE, Walter P. Oligomerization and phosphorylation of the Ire1p kinase during intracellular signaling from the endoplasmic reticulum to the nucleus. EMBO J. 1996;15(12):3028–39.
15. Liu Y, Adachi M, Zhao S, Hareyama M, Koong AC, Luo D, et al. Preventing oxidative stress: a new role for XBP1. Cell Death Differ. 2009;16(6):847–57.
16. Lee AH, Iwakoshi NN, Glimcher LH. XBP-1 regulates a subset of endoplasmic reticulum resident chaperone genes in the unfolded protein response. Mol Cell Biol. 2003;23(21):7448–59.
17. Kim R, Emi M, Tanabe K, Murakami S. Role of the unfolded protein response in cell death. Apoptosis. 2006;11(1):5–13.
18. Xu C, Bailly-Maitre B, Reed JC. Endoplasmic reticulum stress: cell life and death decisions. J Clin Invest. 2005;115(10):2656–64.
19. Woo KJ, Lee TJ, Lee SH, Lee JM, Seo JH, Jeong YJ, et al. Elevated gadd153/chop expression during resveratrol-induced apoptosis in human colon cancer cells. Biochem Pharmacol. 2007;73(1):68–76.
20. Yamaguchi H, Wang HG. CHOP is involved in endoplasmic reticulum stress-induced apoptosis by enhancing DR5 expression in human carcinoma cells. J Biol Chem. 2004;279(44):45495–502.
21. Stewart BW, Wild CP. World cancer report 2014. The International Agency for Cancer Research, France: World Health Organization; 2014. Chapter 5.12.
22. Han QB, Song JZ, Qiao CF, Wong L, Xu HX. Preparative separation of gambogic acid and its C-2 epimer using recycling high-speed counter-current chromatography. J Chromatogr A. 2006;1127(1–2):298–301.
23. Puthalakath H, O'Reilly LA, Gunn P, Lee L, Kelly PN, Hughes PD, et al. ER stress triggers apoptosis by activating BH3-only protein Bim. Cell. 2007;129(7):1337–49.
24. Moon DO, Park SY, Choi YH, Ahn JS, Kim GY. Guggulsterone sensitizes hepatoma cells to TRAIL-induced apoptosis through the induction of CHOP-dependent DR5: involvement of ROS-dependent ER-stress. Biochem Pharmacol. 2011;82(11):1641–50.
25. Selimovic D, Ahmad M, El-Khattouti A, Hannig M, Haïkel Y, Hassan M. Apoptosis-related protein-2 triggers melanoma cell death by a mechanism including both endoplasmic reticulum stress and mitochondrial dysregulation. Carcinogenesis. 2011;32(8):1268–78.
26. Ye J, Rawson RB, Komuro R, Chen X, Davé UP, Prywes R, et al. ER stress induces cleavage of membrane-bound ATF6 by the same proteases that process SREBPs. Mol Cell. 2000;6(6):1355–64.
27. Novoa I, Zeng H, Harding H, Ron D. Feedback inhibition of the unfolded protein response by GADD34-mediated dephosphorylation of eIF2α. J Cell Biol. 2001;153(5):1011–22.
28. Hasegawa A, Osuga Y, Hirota Y, Hamasaki K, Kodama A, Harada M, et al. Tunicamycin enhances the apoptosis induced by tumor necrosis factor-related apoptosis-inducing ligand in endometriotic stromal cells. Hum Reprod. 2009;24(2):408–14.
29. Shinjo S, Mizotani Y, Tashiro E, Imoto M. Comparative analysis of the expression patterns of UTR-target genes caused by UPR-inducing compounds. Biosci Biotechnol Biochem. 2013;77(4):729–35.
30. Wang G, Yang ZQ, Zhang K. Endoplasmic reticulum stress response in cancer: molecular mechanism and therapeutic potential. Am J Transl Res. 2010;2(1):65–74.
31. Schonthal AH. Endoplasmic reticulum stress: its role in disease and novel prospects for therapy. Scientifica (Cairo). 2012;2012:857516.
32. Clarke HJ, Chambers JE, Liniker E, Marciniak SJ. Endoplasmic reticulum stress in malignancy. Cancer Cell. 2014;25:563–73.
33. Liu N, Huang H, Liu S, Li X, Yang C, Dou QP, et al. Calcium channel blocker verapamil accelerates gambogic acid-induced cytotoxicity via enhancing proteasome inhibition and ROS generation. Toxicol In Vitro. 2014;28(3):419–25.
34. Liu N, Huang H, Xu L, Hua X, Li X, Liu S, et al. The combination of proteasome inhibitors bortezomib and gambogic acid triggers synergistic cytotoxicity in vitro but not in vivo. Toxicol Lett. 2014;224(3):333–40.
35. Krajewski S, Tanaka S, Takayama S, Schibler MJ, Fenton W, Reed JC. Investigation of the subcellular distribution of the Bcl-2 oncoprotein: residence in the nuclear envelope, endoplasmic reticulum, and outer mitochondrial membranes. Cancer Res. 1993;53(19):4701–14.
36. Annis MG, Yethon JA, Leber B, Andrews DW. There is more to life and death than mitochondria: Bcl-2 proteins at the endoplasmic reticulum. Biochim Biophys Acta. 2004;1644(2–3):115–23.
37. Szegezdi E, Macdonald DC, Ní Chonghaile T, Gupta S, Samali A. Bcl-2 family on guard at the ER. Am J Physiol Cell Physiol. 2009;296(5):C941–53.
38. Weston CR, Lambright DG, Davis RJ. MAP kinase signaling specificity. Science. 2002;296(5577):2345–97.
39. Urano F, Wang X, Bertolotti A, Zhang Y, Chung P, Harding HP, et al. Coupling of stress in the ER to activation of JNK protein kinases by transmembrane protein kinase IRE1. Science. 2000;287(5453):664–6.
40. Liu D, Zhang M, Yin H. Signaling pathways involved in endoplasmic reticulum stress-induced neuronal apoptosis. Int J Neurosci. 2013;123(3):155–62.